



MASTERARBEIT / MASTER'S THESIS

Titel der Masterarbeit / Titel of the Master's Thesis

“Variations in the gland cells of the pedal surface in
Helix pomatia (Helicidae), *Cepaea hortensis* (Helicidae)
and *Arion vulgaris* (Arionidae) –
A COMPARISON”

verfasst von / submitted by
Sophie Greistorfer (BSc)

angestrebter akademischer Grad / in partial fulfilment of the requirements for the degree of
Master of Science (MSc)

Wien, 2016 / Vienna 2016

Studienkennzahl lt. Studienblatt/
degree programme code as it appears on
the student record sheet:

A 066 831

Studienrichtung lt. Studienblatt/
degree programme as it appears on
the student record sheet:

Master Zoology

Betreut von / Supervisor:

Ao. Univ.-Prof. i. R. Dr. Waltraud Klepal

Mitbetreut von / Co-Supervisor:

TABLE OF CONTENTS

1 ABSTRACT.....	2
2 INTRODUCTION.....	3
3 MATERIAL AND METHODS.....	5
3.1 Specimens.....	5
3.2 Histology and histochemistry.....	5
3.3 Lectin labelling and confocal laser scanning microscopy.....	6
3.4 μ CT imaging.....	7
3.5 Scanning electron microscopy.....	7
3.6 Energy Dispersive X-ray Spectroscopy (EDX).....	7
3.7 Transmissions electron microscopy.....	7
3.8 Evaluation.....	8
4 RESULTS.....	9
4.1 <i>Arion vulgaris</i>	9
4.2 <i>Helix pomatia</i>	13
4.3 <i>Cepaea hortensis</i>	16
5 DISCUSSION.....	20
5.1 <i>Arion</i> gland system.....	20
5.2 <i>Helix</i> gland system.....	21
5.3 <i>Cepaea</i> gland system.....	22
5.4 Comparison of Arionidae and Helicidae.....	23
5.5 Muscular involvement in glandular secretion, dorsal and ventral.....	25
5.6 Summary.....	25
5.7 Outlook.....	26
6 ACKNOWLEDGMENTS.....	28
7 REFERENCES.....	29
8 ABBREVIATIONS.....	33
9 TABLES.....	34
10 FIGURE LEGENDS.....	38
11 FIGURES.....	47
12 APPENDIX.....	69
12.1 Zusammenfassung.....	70

1 ABSTRACT

Gastropods produce high amounts of mucus, which is used in different ways: Defense, adhesion, locomotion or lubrication are only a few of them. As a consequence, several secretory gland types and different chemical composition of their secretion are present particularly in the pedal region of the foot. Although much is known about the glands in this animal group, a comparison of the different glands in terrestrial gastropods is still missing.

In this study a comparison of the morphology of the pedal glands in *Arion vulgaris*, *Helix pomatia* and *Cepaea hortensis* is made using micro computed tomography, histochemistry, ultrastructure and immunocytochemistry. Focus is laid on the gland locality and appearance as well as on the chemical nature of the different gland secretions in each species and results are compared between the species.

The results show a great variety in the arrangement of the different cell types and the mucus composition within and between the species: In the dorsal pedal region of the foot of *Arion vulgaris* five gland types can be distinguished. These contain acidic proteins (positive Alcian blue staining) but lack sugars (negative PAS staining). In the ventral pedal region only four gland types are visible and here acidic mucopolysaccharides are detected.

In *Helix pomatia* three gland types are present in the dorsal region of the foot. They could be distinguished by their reactivity to the different histochemical stainings. In the ventral region only two gland types could be detected also reactive to acidic mucopolysaccharides.

Characterization of the dorsal foot region of *Cepaea hortensis* reveals four different glands, three of them react positively for sugars and acidic proteins while the fourth gland type shows no positive staining at all. The ventral pedal region includes two different gland types, positive for sugar only resp. acidic mucopolysaccharides.

Differences exist between the species regarding the number of glands and content, however the results also show similarities of some glands in the different species.

The question arises whether this variation in the chemistry of the secretory material and mucus composition is the result of different functions and/or related to different living conditions of the animals. Further it will be interesting to find out whether the distribution of the pedal glandular system is related to the presence of a shell.

2 INTRODUCTION

Many diverse animals and plants use adhesives for wide fields of application and scientists are interested to mimic these glues for medical and/or industrial applications (Davies & Hawkins, 1998; Millar et al., 2009; Mostaert et al., 2006). Gastropods are a very promising group, due to its large diversity, the different usage of their glue (defense, adhesion, locomotion or lubrication) and their different habitats (terrestrial, fresh- and saltwater) (Smith, 2006; Smith, 2010). Within the past years, most research has been done on **marine gastropods** as limpets and periwinkle snails, which synthesize predominantly proteinogenic gel-like adhesives. These animals are known for living in harsh areas, such as the intertidal zone (Chapman & Underwood, 1996; Smith, 1992), where a strong adhesive is necessary to provide a stable bonding on different substrata against varying environmental conditions (Smith, 2006) as well as protection against predators (Hahn & Denny, 1989). Beside this strong bonding secretions, another non-adhesive type of mucus is produced for movement (Smith et al., 1999; Smith, 1991). However, the animals are able to vary the composition of the secretion. The mucus used for locomotion lacks a protein, while it is present in the glue for temporary bonding (Smith, 2002; Pawlicki et al., 2004).

Beside marine species also **terrestrial gastropods** produce mucus for similar usage: *Helix aspersa*, for example, survives unfavorable dry periods by forming an epiphragm against moisture loss. This calcareous structure is made from mucus, secreted from mantle collar glands, and becomes strengthened with calcium carbonate (Campion, 1961; Barnhart, 1983). Altogether eight gland types have been distinguished morphologically and chemically in this species. All glands are unicellular and lie in connective tissue, located below the epithelium, but only half of them (subsequently named by the author (Campion, 1961) gland type A, B, C and D) are proposed to be involved in mucus production: Gland type A and B appear in the region of the mantle collar, the dorsal and ventral surface of the foot whereas type A is more common than type B. Although both gland types contain primarily acidic mucopolysaccharides, the secretory material of type A is not granulated, while gland type B has a significant and regular granulation (Campion, 1961). The sole region is dominated by aggregates of gland type C, which contains well defined granulated material. Gland types A, B and C show likewise a weak positive reaction to the PAS and Alcian blue staining, however in the secretory material of type C the protein ratio seems to be higher than in the former two glands. Gland type D is similar to type C concerning their secretory content and staining but less frequently present in the sole. Beside the four mucus-producing glands, the other detected glands contain 1) calcium salt, 2) proteins, 3) fatglobules or 4) flavones. All these types can be

found in the mantle collar and in the dorsal and lateral area of the foot. They differ morphologically by their size and secretory content. The function of these glands varies, either they serve as protection against moisture loss, for defense or they may be related to pigmentation (Campion, 1961).

Arion vulgaris, *Arion subfuscus* and *Ariolimax columbianus* in contrast, lack a protective shell and therefore secrete an extremely stiff mucus when threatened by predators (Martin & Deyrup-Olsen, 1986; Mair & Port, 2002). However this mucus is not as viscous as the one used for locomotion (Deyrup-Olsen et al., 1983). Investigations of *Arion vulgaris* and *Arion rufus* revealed 4 different regions of the body surface, each with specific glands (Wondrak, 2012): There is a protein gland region located on the anterior part of the foot, where neutral mucosubstances are presumed. In the supra-pedal gland region acidic glycosaminoglycans are noted. Another region is located on the ventral surface of the head, where again neutral mucosubstances are present, and a fourth is on the ventral surface of the anterior part of the mantle. In the last one acid mucosubstances are detected. Within this study no explicit differences between the species were noted (Wondrak, 2012).

However, while much attention has been paid to the gastropod species *Helix* and *Arion*, no further details about the mucus production and gland structure seem to be available for the white-lipped snail *Cepaea hortensis*.

The mechanism of mucilage discharge could not be explained exactly for all three species. In some cases in *Helix pomatia* a net of muscles surrounding the cells as part of the releasing mechanism was observed. In other glands no muscles are found and pressure changes in the haemocoel cavity might result in gland secretion (Campion, 1961).

Although numerous studies were made, most of them about the chemistry of the secreted material, it is hard to relate these data to the different species, especially with regard to the releasing mechanism of the gland cells.

The aim of this study is to provide a morphological comparison of the glandular system on the body surface in the three species *Helix pomatia*, *Arion vulgaris* and *Cepaea hortensis*. Similarities in gland morphology as well as mucus composition between the two families Helicidae and Arionidae will be elucidated on histological as well as on ultrastructural level. Furthermore, methods like micro-CT or CLSM, serve to provide better understanding of the gland morphology.

3 MATERIAL AND METHODS

3.1 Specimen

Specimens of *Cepaea hortensis* and *Arion vulgaris* were sampled in the region of Lower Austria (GPS data: N48°4'55.35"; E15°28'50.34"), while individuals of *Helix pomatia* were provided from the snail farmer Andreas Gugumuck (www.wienerschnecke.at). The identification of *Cepaea hortensis* was based on anatomical characteristics. For the present study only adult specimens were considered. In both helicid species the foot was separated from the rest of the body and used for the subsequent morphological analyses.

3.2 Histology and histochemistry

Samples were prefixed for two minutes in an acetic-alcohol-formalin (AFF) solution (Böck, 1989) or in Carnoy's solution (Kiernan, 1999), cut into small pieces and immersed in the respective fixative solution for 3 hrs at room temperature.

Subsequently, the pieces were dehydrated in an ethanol series from 70 – 100 %, cleared with methyl benzoate three changes, 20 min. each and with benzene for 10 min. and finally embedded in paraffin for 12 hrs at 60°C. Serial sections (7µm thick) were made by using a Leica RM2265 rotary microtome (Leica Biosystems GmbH, Nussloch, Germany). Serial sections of 150µm of *Arion vulgaris* were interrupted by gaps (each 150µm) due to the animal length. The sections were mounted on glass slides, using Ruyter's solution (Ruyter, 1931) and dried afterwards.

In addition to tissue sections, mucus from the foot sole was collected on glass slides (smear test) and used for the analyses:

To get morphological overview of the different body wall regions, Azan trichrome (Kiernan, 1999) and Safranin-O (Böhm & Oppel, 1919) stainings were used. To provide evidence of neutral hexose sugar units in the glands, the histochemical staining method PAS (periodic acid – Schiff) (Böhm & Oppel, 1919; McManus & Mowry, 1960) was used, with acetylation (Böhm & Oppel, 1919; McManus & Mowry, 1960) as negative control.

Alcian blue G8X (McManus & Mowry, 1960) staining at the pH-levels 1.0 and 2.5 and Toluidine blue O (in 0.2 M acetate buffer at pH-level 4.3 according to Mulisch & Welsch, 2010) staining was made to differentiate neutral from acidic proteins. To test which glands react positive for acidic mucopolysaccharides, PAS reaction was combined with the Alcian blue staining (McManus & Mowry, 1960).

Biebrich Scarlet at the pH-levels 6.0, 8.0, 9.5 and 10.5 (pH 6.0 in phosphate buffer; Spicer & Lillie, 1961, the other three pH-levels in Laskey's glycine buffer Kiernan, 1999) was used to

detect basic proteins in the tissue. To verify the presence of L-3,4-dihydroxyphenylalanine (L-DOPA) in gastropod mucus, the Arnow staining (Arnow, 1937) was performed on glass slides, with samples of the tube-dwelling polychaete *Sabellaria alveolata* as positive control (Becker et al., 2012).

Lipids in the mucus were visualized with Sudan black (Böck, 1989) on dried mucus smear samples only.

To visualize calcium packages in the body wall Alizarin red S (Kiernan, 1999) as well as von Kossa method (Sheehan & Hrapchack, 1980) were applied.

All staining processes took place at room temperature.

Until now it is not possible to correlate the histochemical results with the ultrastructural data, because most of the granules are too small and so they are not clearly visible on the histochemical sections. Therefore the glands on the figures are in most cases classified as gland type (gt). The gland types C2d and C3d in particular could not be differentiated. So for an easier reading and figure labeling the synonym “C2d/C3d” will be used, which means that “either ... or” resp. “both” gland types are meant.

3.3 Lectin labelling and confocal laser scanning microscopy

All animals were prefixed in 4% PFA (paraformaldehyde) in PBS (phosphate buffered saline, 0.1 M, pH 7.4) and dissected for vibratome sectioning. The pieces were fixed again for 2 hrs at room temperature, using the same fixative. After three washing steps in PBS for 30 min. the samples were embedded in albumin-gelatine, fixed over night in 4% formalin and washed several times in aqua bidest. Serial sections (100µm thick) were made with a vibratome (Leica VT 1200S, Leica Biosystems GmbH, Nussloch, Germany) (for details see protocol Wollesen et al., 2009, 2010).

For a precise determination of the carbohydrates the sections were incubated with fluorescence-labeled lectins: FITC-labeled concanavalin agglutinin (ConA) (EY Laboratories, San Mateo, CA), specific for α -D-mannose/ α -D-glucose; Texas Red-labeled peanut agglutinin (PNA), specific for lactose/ β -galactose; TRITC-labeled soybean agglutinin (SBA) (EY Laboratories, San Mateo, CA), specific for N-acetyl-D-galactosamine; FITC-labeled wheat germ agglutinin (WGA) (EY Laboratories, San Mateo, CA), specific for N-acetyl-D-glucosamine, TRITC-labeled *Galanthus nivalis* lectin (GNA) (EY Laboratories, San Mateo, CA), specific for mannose, and FITC-labeled *Ulex europaeus* agglutinin (UEA), specific for α -L-fucose (see protocol von Byern et al., 2011).

All lectins were diluted in their respective buffers and the sections were stained at a concentration of 1:100 for 30 min at room temperature according to the manufacture protocol

(see for details the EY Laboratories, USA). As negative control the vibratome sections were incubated in the actual buffer solution in the absence of the lectin conjugates.

To visualize muscles and nerves in the mantle epithelia, the sections were stained with 2.5% Alexa Flour TRITC-conjugated phalloidin (R415 Invitrogen Carlsbad, USA) and 1:100 diluted acetylated α -tubulin (T-6793 Sigma-Aldrich St. Louis, USA) with FITC-labeled secondary antibody (M308012 Invitrogen Carlsbad, USA) (see protocol Wollesen et al., 2009, 2010). For orientation the sections were incubated additively with DAPI (D21490 Invitrogen Carlsbad, USA) and observed with a Leica CLSM (TCS SP5X, Leica Microsystems GmbH, Wetzlar, Germany).

3.4 μ CT imaging

After preparation the samples were fixed for 6 hrs at room temperature in Carnoy solution (Kiernan, 1999) and washed several times in 100% ethanol. Subsequently, the samples were contrasted in 1% (w/v) phosphotungstic acid in 70% ethanol for 8 days, afterwards washed and stored in 100% ethanol for the scan. μ CT scans were made from *Arion vulgaris* using an Xradia MicroXCT system and from *Helix pomatia* using a Scanco Medical μ CT 35.

3.5 Scanning electron microscopy

Whole animals were frozen in liquid nitrogen and freeze-dried (Mod. LyovacGT2, Leybold-Heraeus GmbH, Cologne, Germany) until completely dehydrated. Afterwards the animals were broken into smaller pieces, coated with gold in a Sputtercoater (Mod. 108 Agar, Agar Scientific Ltd, Stansted, United Kingdom) and observed with a Philips XL20 (FEI and Philips, Eindhoven, NL).

3.6 Energy Dispersive X-ray Spectroscopy (EDX)

For this study, mucus from the dorsal and ventral mantle epithelium was collected on standard alu-stubs, consisting of aluminium and copper, (Co. Gröpl, Tulln, Austria), airdried and observed with a Jeol T300 equipped with an energy dispersive X-ray spectrometer with a lithium - drifted silicon detector crystal. For evaluation the software program EDAX Team (Software Team, Version 4.3, Co. Ametek Germany) was used. The collecting time of the elements in the mucus was 30s for the selected areas and 100s for dotmapping, both with ~30% dead time.

3.7 Transmission electron microscopy

The animals were prefixed in 2.5% glutaraldehyde with 0.1 M sodium cacodylate buffer (pH 7.4). For ultrathin sections pieces of the ventral and the dorsal side of each animal were

selected and fixed in the same solution for 5 hrs at room temperature. Afterwards the samples were washed three times, ten minutes each in buffer, post-fixed in 1% osmium tetroxid (again in 0.1 M sodium cacodylate buffer at pH 7.4) for 1 hr. After step-wise dehydration samples were infiltrated and finally embedded in epon epoxy resin (AGAR 100, Agar Scientific Ltd, Stansted, United Kingdom). Polymerization took place at 60°C for three days.

Semi-thin sections (1µm thickness) were made with a Leica UC7 microtome (Leica Microsystems GmbH, Wetzlar, Germany) and stained with Toluidine blue. For documentation a light microscope (Model BX41 Olympus, Olympus Corporation, Tokyo, Japan) was used.

Ultrathin sections (70nm thick) were made with an ultra-diamond knife (Diatome AG, Switzerland) on a Leica UC7 microtome and mounted on copper grids.

They were observed with a Zeiss Libra 120 electron microscope (Carl Zeiss AG, Oberkochen, Germany).

3.8 Evaluation

The naming of the gland cells is the same for all three species and common in literature (Smith, 2006). The first letter of the name, a number and acronym “d” for dorsal or “v” for ventral.

To visualize the glands in the dorsal and ventral epithelium a schematic drawing was made using Illustrator CS6 (Adobe Systems, San Jose, USA). All measurements, including the gland dimension, were made with Photopshop CS6 (Adobe Systems, San Jose, USA). The gland length was measured on semithin sections (1µm), the granules within the glands and the dimensions/height of the epithelia were measured on ultrathin sections (70nm thick). To give a good overview and compare the glands/species to each other measurements (six for each information) of the glands/granules were made. To keep the measurement inaccuracy low, only glands with an open duct were measured. A detailed statistic evaluation is missing, because the gland size in different body regions varied a lot and it was not possible to get sufficient measurements.

Videos of *Arion vulgaris* movements were made with a Nikon Coolpix P300. Reconstructions of the muscle network were made with Amira 5.3.3 (Zuse Institut Berlin, FEI Visualization Sciences Group).

4 RESULTS

4.1 *Arion vulgaris*

All gland types of *A. vulgaris* are unicellular, subepithelial and embedded in connective tissue (Fig.1 A). Their nucleus is situated laterally or centrally in the basal area of the gland (Fig.2 A&B). The dorsal epithelial layer achieves a dimension up to $\approx 16\mu\text{m}$, while the ventral is $\approx 22\mu\text{m}$ high. A cilium border, including a microvilli layer, (see labeled areas in Fig.1 A) is located in the ventral region of *Arion vulgaris*, while on the ventral as well as on the dorsal epithelium a microvilli layer (height: $\approx 0.5\mu\text{m}$; Fig.1 A) could be observed. The cilia emerge in the big groove in the transition zone and reach a length of $\approx 11\mu\text{m}$. In the peripheral zone of the ventral side are microvilli but no cilia. This is the part of the foot of the slug which clings to different types of slippery substrata.

Dorsal gland morphology

Semithin and ultrathin sections display five different types of subepidermal glands dorsal on the body wall (A1d, A2d, A3d, A4d, A5d) and one gland type (At) in the transition region (Fig.1 A; Fig.2 A). The glands differ in their appearance, size and secretory content.

A1d is a very common gland type, frequently present in the dorsal area of *Arion* (Fig.1 A; Fig.2 A), extending from the depth of $\approx 158\mu\text{m}$ to the surface. This gland type has a drop-like shape; its secretory material is densely packed and looks like “ice floes” (size around $\approx 3\mu\text{m}$ in the longest dimension) (Fig.4 A; Fig.3 A&C). The granules are homogeneous, however, fixation artifacts may cause a sponge-like appearance of the granular content (Fig.5 A&C). Observations indicate that the secretory material is extruded completely at once (Fig.4 A).

Gland type **A2d** is about $\approx 122\mu\text{m}$ long and likewise a very common gland type in the dorsal body wall (Fig.1 A; Fig.2 A). Although its size and shape is similar to A1d, the secretory content of this gland type differs from that of A1d by having fine granular material between the granules of different size (from $\approx 0.1\mu\text{m}$ up to $\approx 0.6\mu\text{m}$) (Fig.3 E; Fig.4 C).

Gland type **A3d** is likewise frequently present in the *Arion* dorsal body wall as the earlier two gland types (Fig.1 A). Anyhow, this third type is smaller ($\approx 63\mu\text{m}$ long) (Fig.2 A; Fig.3 A) and synthesizes spherical granules (\varnothing from $\approx 0.3\mu\text{m}$ to $\approx 0.8\mu\text{m}$). The granules are easily recognizable as they always have a frayed-like appearance, several concentric rings and an electron-lucent centre (Fig.4 A). In this study the glands appear always filled with granules, but not as densely as for example in A1d.

Only few cells of gland type **A4d** are located in the dorsal region (Fig.1 A; Fig.2 A). This slender gland contains granules of nearly the same size ($\approx 2\mu\text{m}$) and homogeneity as A1d

(Fig.4 B). The granules are tightly packed so that they appear polygonal in the light microscope. The length of this gland type is $\approx 48\mu\text{m}$ (Fig.2 A; Fig.3 C).

A5d differs from the other glands by containing finer granular material (Fig.4 D). The secretory product appears fine and homogeneous (Fig.3 A). Like A1d the gland is large (length $\approx 161\mu\text{m}$) and commonly distributed in the dorsal epithelium (Fig.1 A; Fig.2 A), but obviously not as frequently as A2d.

The gland type **At** could only be observed in the transition region between the dorsal and ventral region (Fig.1 A, Fig.2 A) next to the beginning of the ciliated zone. With a length of $\approx 38\mu\text{m}$ the gland type **At** is the smallest gland type found in the outer region of *Arion*. Its secretory material is organized in roundish granules ($\varnothing \approx 1\mu\text{m}$) (Fig.3 B), which merge and become denser near the apical area (Fig. 4E).

Dorsal gland histochemistry

As mentioned in the method section, it is difficult to assign the staining results to the respective gland types, because some of the granules are very small and can only be differentiated at high resolution (Fig.6).

It is obvious that secretory material of one or more of the large gland cells (A1d, A2d, A5d) provides a weak reactivity to sulfated proteins (Alcian blue staining at pH 1.0; Fig.6 C). However some of the subepidermal gland types show a strong positive reaction to carboxylated proteins (Alcian blue pH 2.5; Fig.6 D) and a gamma metachromasia to Toluidine blue staining at pH 4.3 (Fig.6 B).

In contrast, the glands on the dorsal surface lack neutral sugars, indicated by the negative PAS staining as well as the negative lectin affinity (Fig.6 A). For one of the smaller gland types (A3d) it is questionable if any applied histochemical tests show a positive reaction (Fig.6 A-F).

Basic proteins (Biebrich scarlet staining) as well as DOPA (Arnow reaction) could not be observed in any of the five dorsal gland types. Also the calcium stainings (Alizarin red S & Kossa) and the Safranin-O staining show no positive reaction in the dorsal glands. For the gland type **At** no reaction at all could be observed as this gland type is too small for a light microscopic evaluation.

The secreted mucus, collected from the dorsal region, shows positive affinity to calcium (Alizarin red S and von Kossa method) and lipids (Sudan black).

Dorsal mucus analyses by EDX

The EDX measurement indicates the presence of carbon (51-57 atom%), nitrogen (11-17 atom%) and oxygen (19-26 atom%) in a high amount in the dorsal mucus (Table 1). For the elements chloride (1-7 and 40 atom%) and potassium (2-8 and 44 atom%) different range values could be measured, as these elements are unevenly distributed on the sample (Fig.9 A-C). Sodium, magnesium, phosphorus, sulfur and calcium are also present, however at a very low concentration. Metals and other elements could not be detected.

Ventral gland morphology

In the ventral body wall only four subepidermal gland types could be identified, named A1v, A2v, A3v and A4v (Fig.1 A; Fig.2 B). A1v, A2v and A3v are frequently present and have almost the same size (A1v \approx 82 μ m, A2v \approx 87 μ m, A3v \approx 75 μ m), whereas A4v is bigger (\approx 127 μ m) but rarely present.

A1v has a bunchy form with a narrow duct passing through the epidermis to the surface of the epithelium (Fig.2 A, Fig.3 F). The granules of this gland are homogeneous in their content (Fig.4 G) and also appear as 'ice-floes' as the granules in A1d, however the granules in A1v are larger in size (\approx 4 μ m).

A2v and A1v are similar of shape and situated next to each other (F.2 A, Fig.3 F). In this gland type the tightly packed granules are roundish (\approx 2 μ m) and contain darker particles in the mostly electron-lucent content (Fig.4 G).

The granules in **A3v** are of the same size (\approx 2 μ m) as in A2v (Fig.3 F, Fig.4 G), although they vary slightly in shape. The appearance of this gland is similar to A1v and A2v.

Gland type **A4v** could only be observed in the peripheral region (area without any cilia) of the ventral side (Fig.1 A). With its ballon-like shape and its narrow duct A4v represents the longest gland type (\approx 127 μ m) in the ventral region of *Arion vulgaris* (Fig.2 A). Its secretory material is finely granular as in A2d and A5d but not as homogeneous or dense as in the two gland types on the dorsal region (Fig.4 F).

Ventral gland chemistry

Different to the reactivity of the dorsal gland types, only one of the smaller ventral gland types (A1v, A2v or A3v) shows a strong affinity to sulfated (Alcian blue, pH 1.0) as well as carboxylated glycoproteins (Alcian blue, pH 2.5) and sugars (PAS staining) (Fig.7 A, C and D). Sugar characterization by lectin analyses indicate a strong binding affinity for fucose (lectin *Ulex europaeus* agglutinin - UEA) in the granular material, in the ducts as well as in the secreted mucus (Fig.8 A and B) of any of the three small gland types. The other applied

lectins (ConA, PNA, SBA, WGA, GNA) provided no clear immunocytochemical reactivity to the secretory material.

The largest ventral gland type (A4v) only showed a positive reaction to calcium staining (Alizarin red S, but not for von Kossa method), while all other applied histochemical stainings provide no reactivity. Some calcium deposits could be found in the ventral subepidermal muscle layer (Fig.7 G).

Generally, Biebrich scarlet, Arnow reaction, and von Kossa produced no staining in any of the ventral gland types.

The secreted mucus, collected from the ventral region, shows a strong positive affinity to calcium (Alizarin red S and von Kossa method) and lipids (Sudan black B; Fig.7 H).

Ventral mucus analyses by EDX

The concentration of the elements is similar to the distribution on the dorsal side. Carbon (19-47 atom%), nitrogen (3-14 atom%) and oxygen (8-40 atom%) are predominantly present (Table 1). Again, for the elements chloride (2-11 and under 0.3 atom%) and potassium (4-14 and under 1 atom%) different values could be measured (Fig.9 D-F), while sodium, magnesium, phosphorus, sulfur and calcium are below detection limit. Metals and other elements are absent in the ventral mucus of *Arion vulgaris*.

Muscle system in the *Arion* foot

A branched muscle network could be observed in the *Arion* dorsal and ventral body wall by Azan staining (Fig.6 & 7 E) as well as by fluorescence staining (Phalloidin labeling). From a central circular and longitudinal muscle layer muscle strands lead through the connective tissue up to the surface of the epidermis. The muscle fibers have strong cross connections between the epithelial furrows, which separate the elevated areas. Subepidermal gland cells are surrounded by this muscle network (Fig.8 C and D).

4.2 Helix pomatia

All five gland types (H1d, H2d, H3d, H1v, H2v) observed in *H. pomatia* are unicellular, subepithelial and embedded in the connective tissue (Fig.10). In each of these gland types the nucleus is situated near the base of the gland (Fig 11 A&B). The dorsal epithelial layer (height: $\approx 16\mu\text{m}$) is thinner than the ventral one (height: $\approx 50\mu\text{m}$), both possess deep infoldings (Fig.16 B).

Only ventrally, next to the microvilli ($\approx 2\mu\text{m}$ long), cilia ($\approx 8\mu\text{m}$ longest expansion) could be observed, which are elongated on the central foot on relation to the outer margin (Fig.10).

Dorsal gland morphology

Three types of subepidermal glands (H1d, H2d and H3d) could be differentiated morphologically and by the chemical nature of their secretion (Fig.10, Fig.11 A, Fig.12 A, Fig.13 A-C, Fig.14 C & E, Fig. 15 A-F and H). All of them are embedded in connective tissue, uniformly distributed and H3d is more abundant than H1d and H2d (Fig.10 A).

Type **H1d** is a large gland, reaching a length of up to $\approx 169\mu\text{m}$. It appears pear-shaped or elongated ovoid (Fig.12 D) and secretes through a wide duct (Fig.11 A). Occasionally, several of these glands are next to each other but mostly they appear solitary (Fig.15 H). The secretory content of this gland has an 'ice floes'-like appearance (Fig.13 B, Fig.14 C) and the granules reach a size around $\approx 3.5\mu\text{m}$.

Gland **H2d** is elongate with a narrow duct (Fig.11 A). The glands extend from a depth of $\approx 198\mu\text{m}$ in the connective tissue up to the surface. Different to H1d the secretory material of H2d bears spherical granules of different size ($\approx 1.5\mu\text{m}$ - $\approx 2.5\mu\text{m}$) (Fig.12 A, Fig.13 A&C, Fig.14 E). It remains uncertain, if the different granules represent two different gland types or just different synthesis stages of the gland content.

Gland type (**H3d**), is similar in shape to gland type H1d, but less bulbous (Fig.11 A). Also the duct seems to be narrower than that of H1d (Fig.11 A). This gland type reaches a length of up to $\approx 208\mu\text{m}$. The secretory content is densely packed, homogeneous and finely-grained (Fig.12 A, Fig.13 A).

Dorsal gland histochemistry

Gland type **H1d** shows a strong reactivity of sulphated (Alcian blue at pH level 1.0) and carboxylated (Alcian blue at pH level 2.5) proteins (Fig.15 C and D), but lacks sugars (negative PAS staining and lectin affinity tests) (Fig.15 A2). The histochemical staining with Toluidine blue at pH 4.3 shows a strong gamma metachromasia (Fig.15 B2), which confirms the presence of acidic proteins within the secretory material. Beside the content of H1d, also

the surrounding tissue exhibits a positive staining for Alcian blue at pH level 1.0 and 2.5 indicating the presence of acidic proteins (Fig.15 B2 – F and H). The Safranin-O staining gives a clear positive reaction for the mucin-like secretory content (light red coloration in Fig.15 H) and the Alizarin red S staining indicates that calcium is present in the tissue surrounding this gland type (Fig.15 G).

The smaller gland type **H2d** shows a strong positive affinity to acidic glycoproteins (Safranin-O, PAS, Alcian blue at both pH levels and Toluidine blue staining) (Fig.15 A1, B1, C, D, E, F and H). Moreover, lectin reactivity indicates the presence of mannose (*Galanthus nivalis* lectin - GNA) and fucose sugars (*Ulex europaeus* agglutinin – UEA) within the secretory material (Fig.17 A and B).

H3d shows no reactivity to any applied histochemical staining and immunocytochemical test. This indicates that none of the tested substances is present inside this gland. However on the semithin sections different staining coloration within the gland might be an effect of density differences within the secretory material (Fig.12 A).

Basic proteins (Biebrich scarlet staining) as well as DOPA (Arnou reaction) could not be observed in any of the three dorsal gland types. Also the von Kossa staining shows no positive reaction.

The secreted mucus, collected from the dorsal region, shows positive affinity to calcium (Alizarin red S and von Kossa method) and lipids (Sudan black).

Dorsal mucus EDX analyses

In the mucus a high amount of carbon (21-45 atom%) and oxygen (11-40 atom%) could be measured (Table 2), while to a lower extent, also nitrogen (3-12 atom%) and potassium (2-14 atom%) were detected. For the two elements chloride (0.4-0.6 and 8-10 atom%) and calcium (0.3-0.8 and 3-21 atom%) again different values could be measured, related to an irregular distribution in the samples (Fig.18 A-C). Other elements like sodium, magnesium, phosphorus and sulfur were below detection limit, metals were lacking.

Ventral gland morphology

On the ventral surface only two subepidermal gland types, named H1v and H2v (Fig.10; Fig.11 B, Fig.12 B, C and F, Fig.13 D-F) could be observed within the connective tissue.

Gland type **H1v** has a long narrow duct and an ovoid body (Fig.11 B). It occurs in great numbers and reaches a length of up to $\approx 71\mu\text{m}$. The content of this gland consists of spherical

granules of different size ($\approx 1\mu\text{m}$ - $\approx 1.5\mu\text{m}$) (Fig.11 B, Fig.12 B, C&F, Fig.13 D-F), which merge before secretion (Fig.12 E, Fig.13 F).

The gland **H2v** is more abundant than H1v, its duct appears narrower than in H1v (Fig.11 B) and the gland is significantly longer ($\approx 132\mu\text{m}$). This gland has a slender, at its base slightly bulbous body and is filled with spherical granules of variable size (Fig.12 F, Fig.13 E&F), slightly larger than those of H1v ($\approx 1.5\mu\text{m}$ - $\approx 2\mu\text{m}$).

Ventral gland histochemistry

Histochemical tests show a strong positive staining reaction for sugars (PAS), acidic proteins (Alcian blue staining at pH 1.0 and pH 2.5, Toluidine blue at pH 4.3) (Fig.16 A-D, F), indicating the presence of acidic glycoproteins for one or both gland types. Further detailed characterization of the sugars by lectin labeling shows moreover a strong specificity for mannose (*Galanthus nivalis* lectin - GNA) and fucose (*Ulex europaeus* agglutinin – UEA) (Fig.17 D&E) as found in the dorsal gland type H2d.

In both ventral gland types basic proteins (Biebrich scarlet staining), calcium (Alizarin red S and von Kossa method) as well as DOPA (Arnow reaction) could not be observed.

The secreted mucus, collected from the ventral region, furthermore shows a strong positive affinity for lipids (Sudan black B; Fig.16 H) and light affinity for calcium (Alizarin red S & von Kossa).

Ventral mucus EDX analyses

The ventral mucus shows some minor variations of the element composition given for the dorsal side (Tab.2). Ventrally, sodium is lacking, instead a very high amount of calcium (10-21 atom% and under 1 atom%) could be measured in some areas (Fig.18 D-F). Mostly common elements are again carbon (19-42 atom%) and oxygen (3-59 atom%), while nitrogen is present in lower concentration (1-4 atom%). As for the dorsal mucus, magnesium, phosphorus, sulfur and potassium values are below detection limit and metals are lacking.

Muscle system in the *Helix* foot

A branched muscle network crosses the entire foot extending from the ventral surface towards the dorsal surface (Fig.16 E, 17 C).

4.3 *Cepaea hortensis*

The observed pedal glands on the dorsal as well as ventral side of *Cepaea hortensis* are unicellular (Fig.19; Fig.20 A & B), embedded subepithelially in the connective tissue. In most cases the roundish nucleus is located in the basal part of the gland, in case of two dorsal glands (C1d and C4d) it appears adjacent to the apical pole of the cell as the glands are tightly filled with secretory material.

The dorsal epithelium has a thickness of $\approx 18\mu\text{m}$, while the ventral one is up to $\approx 40\mu\text{m}$ thick. Beside the thickness another conspicuous difference between the dorsal and the ventral side in *Cepaea* is a rim of cilia (up to $\approx 4\mu\text{m}$ cilium length), including a microvilli layer, on the ventral side, whereas in the dorsal region are only microvilli ($\approx 1.5\mu\text{m}$ microvilli length).

Dorsal gland morphology

In the dorsal region of the *Cepaea* pedal system four gland types (subsequently named C1d, C2d, C3d and C4d) could be distinguished (Fig.20 A) by their location and granular content (Fig.21 A, B & C; Fig.22 A - C, F&G; Fig.23 A - E). While C1d and C4d are the most common gland types, glands C2d and C3d appear rarely (Fig.20 A).

C1d is a large gland, with a length of $\approx 256\mu\text{m}$ (Fig.20 A). The gland is club-shaped and possesses a wide duct (Fig.21 C; Fig.22 A). The secretory material consists of densely packed, ice floes-shaped granules ($\varnothing \approx 8\mu\text{m}$) with a grained structure (Fig.22 A & F; Fig.23 B).

Gland type **C2d** (Fig.20 A; Fig.21 A; Fig.22 B & F) has a length of $\approx 69\mu\text{m}$. It is elongated pear-shaped and possesses a narrow duct. The secretory content of the spherical granules consists of fine grained material ($\approx 2\mu\text{m}$) with small electron-dark inclusions (Fig.19; Fig.22 F).

C3d is similar in shape and length ($\approx 74\mu\text{m}$) to C2d (Fig.20 A; Fig.21 A). However, the homogeneous granular material ($\approx 2\mu\text{m}$) of C3d appears generally more electron-dense than that of C2d and lacks inclusions.

The fourth gland type (**C4d**) (Fig.20 A; Fig.21 B; Fig.22 C) is similar to C1d club-shaped, however it is more slender and has a narrow duct. With a height of $\approx 325\mu\text{m}$ C4d is the largest dorsal gland in *Cepaea*. The secretory material consists of densely packed, fine grained material (Fig.19; Fig.21 B; Fig.22 C).

Dorsal gland histochemistry

The secretory content of gland type **C1d** consists of acidic glycoproteins (strong positive reaction to PAS and Alcian blue at both pH levels as well as to Safranin-O staining) (Fig.24 A, C, D and F), however no specific affinity for any tested lectin could be observed. Further

characterization with Toluidine blue shows, that the acidity of the proteins extend to a pH level of 4.3 (Fig.24 B). Beside the secretory material, also the tissue, surrounding the gland type, stains positive for glycoproteins (Fig.24 A-D). Furthermore, calcium could be detected in the surrounding area (positive Alizarin red S staining) (Fig.26 B).

Due to the similar appearance and secretory composition it was impossible on histochemical level to distinguish gland types **C2d** and **C3d** by light microscopy. Nevertheless, two different gland types could be differentiated ultrastructurally:

The secretory material of one gland type (dedicated as **C2d/C3d**) likewise reacts, as C1d, strongly to PAS and Alcian blue (pH level 1.0 and 2.5) (Fig.24 A, C and D), as well as with Toluidine blue (metachromatic staining into red-purple colour). Moreover, also basic proteins at a pH level of 8.5 only (Biebrich scarlet staining) (Fig.26 A) could be detected, while no reaction is given for the other pH values. Detailed characterization of the sugar components in the glandular material indicates a high affinity for mannose (*Galanthus nivalis* lectin - GNA) (Fig.27 A).

The other gland type (either **C2d/C3d**) shows a slightly weaker reaction to PAS and Alcian blue staining and no affinity to basic proteins (Biebrich scarlet staining) at any pH level.

C4d does not react to any of the applied histochemical staining and immunocytochemical reactions.

Beside the presence of mannose sugars (lectin GNA) in C2d or C3d only, other sugar residuals as α -L-fucose (lectin UEA), N-acetyl-D-glucosamine (lectin WGA) and a-D-mannose/a-D-glucose (lectin ConA) are present in the dorsal integument. However, so far it is not possible to assign the data to the secretory material of any of the four gland types.

The Arnow reaction (DOPA) as well as the von Kossa method provides no reaction to any dorsal gland.

The secreted mucus, collected from the dorsal region, shows positive affinity to calcium (Alizarin red S and von Kossa method) and lipids (Sudan black).

Dorsal mucus EDX analyses

The EDX measurements indicate a high amount of carbon (20-34 atom%), oxygen (9-37 atom%), chloride (8-27 atom%) and potassium (8-28 atom%) in the dorsal mucus (Table 3), to a lower extent also nitrogen (4-10 atom%). Other elements (i.e. sodium, magnesium, sulfur and calcium) are below the detection limit and metals are lacking. An irregular distribution of

some elements (chloride, potassium) could be documented through dot mapping analyses (Fig.28 A-C).

Ventral gland morphology

The ventral surface in *Cepaea* shows significant differences to the dorsal side (Fig.20 B), by having only two gland types (C1v and C2v). The epithelium consists of a non-glandular cell type with clear visible deposits.

Gland type **C1v** is elongated with a length of $\approx 107\mu\text{m}$, club-shaped with a narrow duct and occurs regularly (Fig.20 B; Fig.21 D; Fig. 26 D). The granules are loosely packed, almost spherical in size with a diameter of $\approx 1\mu\text{m}$ and are embedded in diffuse finely grained material. Near the apical pole of the gland the granules merge before extrusion (Fig.22 D). These granules are electron dense with electron lucent inclusions (Fig.19).

Gland type **C2v** is rarely present (Fig.19) in the ventral foot epithelium. With its length ($\approx 113\mu\text{m}$) and appearance it is similar to C1v. However, the granular material of C2v is more densely packed and electron-lucent (Fig.21 D, Fig. 22 E), homogeneous in its structure and slightly larger in size ($\approx 1\mu\text{m}$). As for C1v also the granules of C2v fuse apically before extrusion (Fig. 22 H).

In the epithelial cells are electron dense **deposits** (Fig.20 B; Fig.22 E), which are almost spherical and in most cases located distally in the cell.

Ventral gland histochemistry

C1v reacts weakly to neutral sugars (PAS reaction) as well as proteoglycans (Safranin-O staining) (Fig.25 F), while the strong Alcian blue (at both pH levels) as well as Toluidine blue reaction indicate the dominance of acidic proteins (Fig.25 A - D, Fig.26 D).

It is not sure if the secretory material of gland type **C2v** does not react to any applied histochemical test, while the deposits of the epithelial cells consists of basic proteins (positive Biebrich scarlet staining at pH level 6.0 and 8.5) (Fig.26 E).

Incubation with *Galanthus nivalis* lectin (GNA) (Fig.27 D) indicates the presence of mannose, but it was not possible to assign it to any of the two ventral glands.

Generally, a reaction to Arnow staining, Alizarin red S and von Kossa method could not be observed for any of the two cell types, while the isolated mucus, shows a light positive reaction for calcium (Alizarin red S and von Kossa reaction) and lipids (Sudan black B, Fig. 26 C).

Ventral mucus EDX analysis

In the ventral mucus carbon (24-47 atom%) and oxygen (12-32 atom%) are prominent (Table 3), to a lower extent also nitrogen (4-15 atom%), chloride (6-16 atom%) and potassium (9-20 atom%). Sodium, magnesium, phosphorus, sulfur and calcium are below detection limit and metals are lacking.

Muscle system in the pedal integument

Labeling with phalloidin confirms the presence of a strong branched muscle net within the dorsal and ventral side of the *Cepaea* foot (Fig.25 E), cross connecting the epithelial infoldings (Fig.27 C).

The muscle fibers, upcoming from the subepithelial tissue, end beneath the epithelium. Observations show that the glands are enclosed by muscle fibers (Fig.27 E; Fig.24 E), however a direct attachment of the muscles at the gland membranes could not be observed in this study.

5 DISCUSSION

5.1 *Arion* gland system

Although this group of gastropods is widespread in Europe and frowned by many garden owners, we still know very little about the glands in this gastropod group: Herfs (1921) defined generally for pulmonates three types of gland cells: 1) the basophile “echte Schleimdrüsen”, which occur mostly in the ventral area and are responsible for mucus production, 2) the “basophile Kalkschleimdrüsen” and 3) acidophile glands, both located in the dorsal region and secreting the calcareous mucus resp. epithelial pigment.

Later, Barr (1927) specified for *Arion ater* three types of gland cells, 1) the “unicellular mucous” glands keeping the skin moist, 2) the “calcic” glands producing defence secretions and 3) the “pigmentary” glands, responsible for the skin pigmentation. However these three gland types were proposed to be present in the dorsal as well as ventral region. In the peripodial groove (the transition zone between the dorsal and ventral mantle margin) Barr (1927) mentioned another gland type, the peripodial gland, which appears to be an aggregation of the first gland type (Barr, 1927).

In *A. rufus* four gland types were described in the ventral region (Chétail & Binot, 1967), while Wondrak (1967) distinguishes by TEM in the same species only three gland types. In both studies no information is given about the number of glands types in the dorsal region.

The present characterization of the gland types in *Arion vulgaris* shows differences to earlier description of Arionid species:

Ventrally in *A. vulgaris* as well as *A. rufus* four gland types could be observed. The secretion of both gland types consists of acidic mucopolysaccharides and lipids (Chétail & Binot, 1967 and present study). However, in *A. vulgaris* furthermore positive reactions are given for calcium (Alizarin red S & von Kossa method), which was not described in *A. rufus*. Dorsally, five gland types are described in *A. vulgaris*, which may correspond to the two gland types described by Herfs (1921) and for *A. ater* by Barr (1927). Unfortunately a clear morphological and histochemical correlation of the present data to those earlier descriptions is not possible at this stage. However, the gland type “At”, found in the transitory zone in *A. vulgaris* (present study) surely corresponds to the peripodial gland, mentioned by Barr (1927) for *A. ater*, but no information is given for *A. rufus* by Chétail & Binot (1967).

Beside the Arionid species in other pulmonate species, like *Lehmania poirieri* (Arcadi, 1967) or terrestrial slugs as *Meghimatium fruhstorferi* (*Incilaria fruhstorferi*) only two gland cells are defined Yamaguchi et al., 2000 in the dorsal and ventral epithelium. In *Meghimatium*

fruhstorferi the 1) round mucous cells are more abundant on the ventral than on the dorsal surface, contrary to the 2) tubular glands (Yamaguchi et al., 2000). Histochemical data indicate that the round mucous glands stain positive for lectin WGA and SBA only, while in the tubular glands are acidic mucopolysaccharides (Yamaguchi et al., 2000). Despite the fact that more gland types are present in *Arion vulgaris*, its composition of the secretion corresponds histochemically to those glands found in *M. fruhstorferi*. In the ventral secretion glycoproteins are present in both species, however with a different lectin affinity (N-acetyl-D-glucosamine and N-acetyl-D-galactosamine in *M. fruhstorferi*; fucose in *A. vulgaris*) (Yamaguchi et al., 2000 and present study). Dorsally, both species bear acidic proteins in addition in *M. fruhstorferi* sugars are found (Yamaguchi et al., 2000 and present study).

5.2 *Helix* gland system

As in *Helix aspersa* (Campion, 1961; Tonar & Markos, 2004), the epithelium of *H. pomatia* contains a single layer of columnar cells. The thickness of the layer varies in the two species (in *H. aspersa* 25-33µm ventrally; in *H. pomatia* 50µm ventrally) (Campion, 1961 and present study).

Differences between the two species are given in view of the number of glands in the dorsal and ventral subepithelium:

For *H. aspersa* eight glands are defined (mucus gland types A, B, C, D, calcium gland, protein gland, pigment gland, lipid gland). Four of them (gland type A-D) are involved in the mucus production (Campion, 1961). In the dorsal region gland type A occur, those 'reticular or bubbly' (original description by the author) secretions react positive to Alcian blue, Neutral red and weak reaction to PAS. Gland type B contains homogeneous granular material, which likewise stains positive for Alcian blue and PAS only. Occasionally, calcium glands containing either pigment or lipids (positive reaction for von Kossa method, Alizarin S red, etc) are present (Campion, 1961).

In the transitory zone between the dorsal and ventral region four gland types, pigment glands, calcium glands, glands type B and lipid glands (lipid globules, positive reaction to Sudan black) are present.

In the ventral region (sole foot) the calcium glands, gland type C and occasionally gland type D are described (Campion, 1961). Gland type C contains distinct reticular granules and stains positive for Alcian blue and PAS as for gland type A. The granules of gland type D are similar to those of gland type C. They stain positive to Alcian blue and PAS, but are not metachromatic with Toluidine blue as for gland type C. However, according to Campion

(1961), it remains questionable whether gland type D is a distinct type or a developmental stage of gland type C.

In the present study on *H. pomatia* three different types of subepidermal glands (H1d, H2d and H3d) could be distinguished in the dorsal area, which contain either acidic proteins (H1d), acidic glycoproteins (H2d) or show no reactivity at all (H3d). In the ventral region of *H. pomatia* the two gland types H1v and H2v show reactivity for acidic glycoproteins.

Correlating the results for both *Helix* species, the dorsal gland type H1d in *H. pomatia* corresponds morphologically and histochemically to gland type A in *H. aspersa*. Gland type A displays a slightly weaker PAS reactivity. Gland type H2d is similar to gland type B in *H. aspersa*. Nevertheless the two gland types in *H. aspersa* are larger than those glands described in *H. pomatia*. In *H. aspersa* gland size differences were noted between the mantle and dorsal foot area (Campion, 1961). The size and chemical content of gland H1v are similar to gland type C in *H. aspersa*. It could not be excluded that gland type H2v described in *H. pomatia* corresponds to the immature gland type D in *H. aspersa*. However, further investigations are necessary to verify this hypothesis.

Beside the similarity of the mucus-producing cells, in the ventral *H. pomatia* mucus also lipids and calcium are detectable, indicating the presence of specific cells as given for *H. aspersa* (Campion, 1961). Further studies are planned to locate the glands in this tissue region.

5.3 *Cepaea* gland system

Up to date no description is given for the mucus-producing gland system in this helioid genus. Comparing the *C. hortensis* gland system with those of *Helix pomatia*, both bear a singular layer of columnar cells in the epithelium. Anyhow, great differences concerning number of gland types and mucus composition exist: In *H. pomatia* are dorsal three gland cells (H1d, H2d, H3d), while in *C. hortensis* four glands (C1d, C2d, C3d and C4d) exist.

In view of its size, secretory content and chemical nature, the gland type H2d (*Helix pomatia*) corresponds to gland type C2d/C3d in *Cepaea hortensis*.

H1d secreting acidic proteins or H3d of *H. pomatia* showing no reactivity to any stainings, have no counterpart in *C. hortensis*. Ventral are in both species two gland types, C1v and C2v in *C. hortensis* resp. H1v and H2v in *H. pomatia*. In *C. hortensis* only C1v reacts positively to acidic glycoproteins, while in *H. pomatia* the two gland types H1v and H2v contain acidic glycoproteins. Moreover, C1v shows only an affinity for mannose, while in the *H. pomatia* glands are also fucose sugars.

Detailed morphological comparison on ultrastructural level of the dorsal and ventral glands in both species is currently in progress to show similarities and differences of the secretory composition and appearance. A detailed study of the other, non-mucus producing glands in both species will also be made.

Beside the difference concerning number of gland types and their different acidic mucus composition the dorsal glands in *C. hortensis* show a positive reactivity for basic proteins (Biebrich scarlet reaction at a pH level 6.0 and 8.5 and other sugars as a-D-mannose / a-D-glucose and N-acetyl-D-glucosamine), but not so in *H. pomatia*.

This difference in mucus composition in both helioid species cannot be explained at present. Both species occur in the same habitat and produce an epiphragma (Kilias, 1985; Fischer & Reischütz, 2008). Further investigations are therefore helpful to verify a chemical adaptation to different predators or a behavioral adaptation.

5.4 Comparison of Arionidae and Helicidae

All three species (*A. vulgaris*, *H. pomatia* and *C. hortensis*) share a similar morphology of the body wall: an outer single epidermal layer and a thicker subepidermal layer, bearing the mucus glands. Moreover, all three investigated species possess a cilium border in the central part of the ventral foot epithelium. This cilia area has already been described earlier for other *Arion* species (Barr, 1927; Chétail & Binot, 1967), and the authors hypothesized that it is used for the distribution of the ventral secretions during locomotion.

Beside the mucus dispersal, the cilia presumably also have a protective function during movement and play a role in adhesion too (Bravo Portela et al., 2012).

Great differences between the two groups are not only seen macroscopically (no shell vs. external shell), the production of the trail mucus differs too:

In the two helioid species the ventral glands are responsible for locomotion of the animal, secreting the so called trail-mucus. This mucus either consists of acidic proteins (in *Cepaea hortensis*) or acidic glycoproteins (in *Helix pomatia*) and sugars as mannose (both species) and additionally fucose (*H. pomatia*). In Arionid species the trail mucus is produced by a so called suprapedal gland system (earlier defined as pedal gland by Barr, 1927), located within in the ventral body cavity and containing one gland type only (Wondrak, 2012). Histochemically, this trail mucus consists of acidic proteins and specific sugars as galactose, N-acetyl-a-D-galactosaminyl and galactose b1-3N-acetyl-galactosamine, but is negative for PAS staining (Wondrak, 2012).

In the two helioid species sugar components could be confirmed in the dorsal gland secretions surely serving to reduce the friction force between the soft skin and the hard shell by

producing a hydrogel-like lubricant (Herfs, 1921). Instead in the dorsal mucus of *Arion vulgaris*, glycoprotein components are absent, indicating another mode of protection against predators or bacteria as discussed earlier (Herfs, 1921; Werneke et al., 2007). Anyhow also in *Helix pomatia* an acidic protein producing gland could be detected. Further studies may be necessary to discuss an involvement of this acidic mucus for defence or higher viscous lubricant for its larger shell.

It is well described that the two Helicidae snails produce and secrete the calcium through a specific gland to build their shell and epiphragm (Barnhart, 1983; Pawlicki et al., 2004), an absence of such glands are therefore coherent for *A. vulgaris*. Interestingly, calcium components could be proven in the ventral gland type A4v and by EDX in the ventral and dorsal mucus secretions. The low calcium amount in the dorsal secretion in the two helicid species may correlate with a low production and shell-building phase during captivity. The animals used in the present study were cleaned before isolating the dorsal and ventral mucus for the EDS-SEM measurements.

It is known that calcium as well as other elements (e.g. potassium, chloride) and/or metals (i.e. iron or copper) are present in the mucus of some terrestrial species (i.e. *Arion subfuscus* Werneke et al., 2007 or *Helix aspersa* Campion, 1961), while other pulmonates (*Limax pseudoflavus* (Cook & Shirbhate, 1983; Shirbhate & Cook, 1987) and *Incilaria fruhstorferi* (Yamaguchi et al., 2000)) lack calcium glands. Also in marine species as *Lottia limatula* only metals as iron could be detected (Smith et al., 1999). These elements are not only involved in the shell formation as given for helicid species but also play a role in the cross-linkage and viscosity of the mucus (Campion, 1961; Deyrup-Olsen et al., 1983; Pawlicki et al., 2004; Werneke et al., 2007) as known and described for the *Mytilus* byssal system (Waite et al., 2005).

Metal elements (iron, copper, manganese) as found in earlier studies on *Arion subfuscus* and *Helix aspersa* (Pawlicki et al., 2004; Werneke et al., 2007) could not be confirmed in the present study in *Arion vulgaris* and *Helix pomatia*. The reason for this may be that in the earlier studies the secretions from a larger number of species (> 30) were isolated and analyzed, resulting in a detectable amount of metal elements in the secretions. Moreover, in the earlier studies razor blades were used to scratch the dried mucus from the aquaria glass, therefore a preparative contamination could not be excluded.

5.5 Muscular involvement in glandular secretion, dorsal and ventral

The subdermal musculature in all three investigated species, *Arion vulgaris*, *Helix pomatia* and *Cepaea hortensis* is similar, showing a highly branched network and strong cross connections between the epithelial furrows. Beside its main function for the animal locomotion, it is also proposed that secretion of the mucus glands is regulated by muscle contraction. In a related study in *H. pomatia* single smooth muscle cells and connective tissue were mentioned around glands (Tonar & Markos, 2004), however its function in mucus discharge is not discussed by the authors. Also in *Incilaria fruhstorferi* as well as *Lymnea luteola* a network of muscle fibers is observed (Yamaguchi et al., 2000; Vijaya kumar et al., 2013) and in *Lymnea stagnalis* six muscle systems can be differentiated in the body wall of the animal (Plesch, 1977). Campion (1961) mentioned for *Helix apersa*, that some gland cells are enclosed in a network of muscle-fibres while others lack muscular connection and may be discharged through haemocoel pressure.

In the present study, in all three species subepidermal mucus glands are embedded in the muscular network, however a direct contact of muscular fibers to the glands could not be observed. In summery, further studies are necessary to find out if all glands are surrounded by the musculature or if muscular contacts to specific gland types are given as observed by Campion (1961).

5.6 Summary

In the present study a characterization of the subepithelial secretory gland types were made in all three gastropod species, focusing on their morphology and gland composition. Since light microscopic resolution is not high enough to define the gland cells, detailed description and distinction is made in particular on ultrastructural level. In Table 4, differences and similarities are highlighted between the gland cells.

In *Arion vulgaris* ten subepithelial gland cells (Table 4) could be differentiated morphologically. Five of the glandular cells are located in the dorsal region, four in the ventral region and one in the transition area in the big groove. It can not be excluded that some dorsal and ventral glands (e.g. A1d and A1v respectively A2d and A5d) are just different stages, however, as the glands differ structurally and in view of their secretory content, this hypothesis is not likely. Here also the histochemical data give no further information. All other glandular cells detected in the *Arion* foot epithelium vary strongly in their granular content and are classified as independent gland types.

In *Helix pomatia* five subepithelial glandular cells (three dorsal and two ventral) were identified (Table 4). Here, the morphological differences in four of the five glandular cells are obvious. Only for gland cell H2d/H2d*, two different gland types or stages of one gland type may occur, based on the structural differences of the secretory content. The present data show that the gland cells always appear next to each other and fused in some cases, speaking for one gland type with developing content. Unfortunately, so far the histochemical data do not support this hypothesis.

In *Cepaea hortensis* six subepithelial glandular cells (four dorsally and two ventrally) were identified (Table 4). For C1d and C4d a clear identification on the basis of the morphological and histochemical results is possible. Contrary to C1d and C4d, C1v and C2v are unique in their morphology and similar in their chemical content (Table 4). However the glands differ ultrastructurally, but a clear chemical differentiation of these two gland types is not possible at this stage as the light-microscopic resolution is insufficient.

Summarizing, the present data indicate that most gland types found in the three gastropod species are clearly unique and not only transitional stages. Nevertheless in some cases, doubts remain and further studies are needed to differentiate these glands and determine their status of maturity.

5.7 Outlook

The present study surely provides only a first insight in the foot glandular system of the three different gastropod species, further investigations have to follow to correlate the histological and ultrastructural data. By this it will be possible to determine the number of gland types involved in mucus production.

The histochemical methods are limited in their possibilities and could provide only a general view of the three macromolecule types (sugars, proteins, lipids) produced in the gland types. Further biochemical investigations need to follow to determine more profound knowledge of the sugar types and proteins present in the mucus glands for all three species and determine similarities and differences in mucus composition also in view of its function (i.e. the antipredator/moisture protective mucus produced dorsally).

Seasonal investigations of the mucus production in *Patella caerulea* point out a change in gland chemistry through different seasons (Petraccioli et al., 2013). As all three species investigated in this study not only cope with higher temperature and humidity conditions, throughout the day and different season, as for the marine species *Patella caerulea* but also hibernate during the winter season underground or in protected areas. A chemical

change/adaptation of the mucus to this varying climate conditions are surely conceivable and need to be investigated more detailed in the future.

Currently, investigations are in progress to determine the usage of snail mucus not only for the cosmetic and beauty industry (creams and face mask products are already available) but for medical applications.

Maybe in future medical adhesives based on snail mucus may be developed as this material is not only very flexible (Smith, 2002), but also adhere perfectly on wet surfaces (Smith, 1991), an important character for surgical applications.

6 ACKNOWLEDGEMENTS

For great care and support during my master thesis, I thank Univ.-Prof.i.R. Dr. Waltraud Klepal. Furthermore, the success of the thesis was only possible with the help of Ao.Univ.-Prof. Dr. Irene Lichtscheidl, which allowed me to use the laboratories and equipment of her department. Many thanks to Dr. Janek from Byern for his active support and encouraging words. Thanks to Mag. Norbert Cyran and Mag. Daniela Gruber for their support, especially in terms of assistance in the use of equipment. Furthermore, I would like to thank Univ.-Prof. DDR. Andreas Wanninger and AR Dr. Livia Rudoll because of the opportunity to use the histochemical laboratory. For its excellent assistance in the ultrastructure (sections and photos) I want to thank Mag. Johannes Suppan. I want to thank the entire CIUS team, especially Dr. Vanessa Zheden, for many friendly words and an open ear. Finally, I owe my loyal and valued friends and my family a great debt of gratitude, for bearing my nagging during an often busy, as well as very exciting time and the many encouraging words.

These investigations were partly funded by the Austrian Science Fund FWF (Project No. AP 24531-B21)

7 REFERENCES

1. Arcadi, J. A. (1967): The two types of mucous gland cells in the integument of the slug, *Lehmania poirieri* (Mabille): a study in metachromasy. Transactions of the American Microscopical Society 86, 506-509.
2. Arnow, L. E. (1937): Colormetric determination of the components of 3,4-dihydroxyphenylalanine-tyrosine mixtures. Journal of Biological Chemistry 118, 531-537.
3. Barnhart, M. C. (1983): Gas permeability of the epiphragm of a terrestrial snail, *Otala lacta*. Physiological Zoology 56 (3), 436-444.
4. Barr, R. A. (1927): Some notes on the mucous and skin gland of *Arion ater*. Journal of Microscopical Science S2 (71), 503-525.
5. Becker, P. T., Lambert, A., Lejeune, A., Lanterbecq, D., and Flammang, P. (2012): Identification, Characterization, and Expression Levels of Putative Adhesive Proteins From the Tube-Dwelling Polychaete *Sabellaria alveolata*. Biological Bulletin 223 (2), 217-225.
6. Böck, P. (1989): Romeis Mikroskopische Technik. München: Urban und Schwarzberg, 1-697.
7. Böhm, A. and Oppel, A. (1919): Taschenbuch der mikroskopischen Technik - Anleitung zur mikroskopischen Untersuchung der Gewebe und Organe der Wirbeltiere und des Menschen unter Berücksichtigung der embryologischen Technik. (Romeis, B. Eds.) München: R. Oldenbourg, 1-437.
8. Bravo Portela, I., Martinez-Zorzano, V. S., Molist-Perez, I., and Molist Gracia, P. (2012): Ultrastructure and glycoconjugates pattern of the foot epithelium of the Abalone *Haliotis tuberculata* (Linnaeus, 1758) (Gastropoda, Haliotidae). The Scientific World Journal 960159, 1-12.
9. Champion, M. (1961): The structure and function of the cutaneous glands in *Helix aspersa*. Quarterly Journal of Microscopical Science 102, 195-216.
10. Chapman, M. G. and Underwood, A. J. (1996): Influence of tidal conditions, temperature and desiccation on patterns of aggregation of the high-shore periwinkle *Littorina unifasciata*, New South Wales, Australia. Journal of Experimental Marine Biology and Ecology 196, 213-237.
11. Chétail, M. and Binot, D. (1967): Particularites histochimiques de la glande et de la sole pedieuses d' *Arion rufus* (Stylommatophora: Arionidae). Malacologia 5 (2), 269-284.
12. Cook, A. and Shirbhate, R. (1983): The mucus producing glands and the distribution of the cilia of the pulmonate slug *Limax pseudoflavus*. Journal of Zoology, London 201, 97-116.
13. Davies, M. S. and Hawkins, S. J. (1998): Mucus from marine molluscs. Advances in Marine Biology 34, 1-71.

14. Deyrup-Olsen, I., Luchtel, D. L., and Martin, A. W. (1983): Components of mucus of terrestrial slugs (Gastropoda). *American Journal of Physiology - Regulatory, Integrative and Comparative Physiology* 245, R448-R452.
15. Fischer, W. and Reischütz, A. (2008): Beiträge zur Kenntnis der österreichischen Molluskenfauna XI. Die Molluskenfauna der Umgebung von Markthof sowie des Stempfelbaches (Marchfeld, NÖ). *Nachrichtenblatt der Ersten Vorarlberger Malakologischen Gesellschaft* 15, 51-55.
16. Hahn, T. and Denny, M. (1989): Tenacity-mediated selective predation by oystercatcher on intertidal limpets and its role in maintaining habitat partitioning by "*Collisella*" *scabra* and *Lottia digitalis*. *Marine Ecology Progress Series* 53 (1), 1-10.
17. Herfs, A. (1921): Die Haut der Schnecken in ihrer Abhängigkeit von der Lebensweise. *Naturwissenschaftliche Wochenschau* 20 (42), 601-609.
18. Kiernan, J. A. (1999): *Histological and histochemical methods: Theory & Practice*. Oxford: Butterworth Heinemann, 1-502.
19. Kiliyas, R. (1985): *Die Weinbergschnecke*. Wittenberg: A Ziemsen verlag, 1-116.
20. Mair, J. and Port, G. R. (2002): The influence of mucus production by the slug, *Deroceras reticulatum*, on predation by *Pterostichus madidus* and *Nebria brevicollis* (Coleoptera: Carabidae). *Biocontrol Science and Technology* 12, 325-335.
21. Martin, A. W. and Deyrup-Olsen, I. (1986): Function of the epithelial channel cells of the body wall of the terrestrial slug *Ariolimax columbianus*. *Journal of Experimental Biology* 121, 301-314.
22. McManus, J. F. A. and Mowry, R. W. (1960): *Staining methods: Histological and Histochemical*. New York: Paul Hoeber Inc., 1-423.
23. Millar, N. L., Bradley, T. A., Walsh, N. A., Appleyard, R. C., Tyler, M. J., and Murrell, G. A. (2009): Frog glue enhances rotator cuff repair in a laboratory cadaveric model. *Journal of Shoulder and Elbow Surgery* 18 (4), 639-645.
24. Mostaert, A. S., Higgins, M. J., Fukuma, T., Rindi, F., and Jarvis, S. P. (2006): Nanoscale mechanical characterisation of amyloid fibrils discovered in a natural adhesive. *Journal of Biological Physics* 32 (5), 393-401.
25. Mulisch, M. and Welsch, U. (2010): *Romeis Mikroskopische Technik*. Heidelberg: Spektrum Akademischer Verlag, 1-551.
26. Pawlicki, J. M., Pease, L. B., Pierce, C. M., Startz, T. P., Zhang, Y., and Smith, A. M. (2004): The effect of molluscan glue proteins on gel mechanics. *Journal of Experimental Biology* 207, 1127-1135.
27. Petraccioli, A., Maio, N., Guarino, F. M., and Scillitani, G. (2013): Seasonal variation in glycoconjugates of the pedal glandular system of the rayed Mediterranean limpet, *Patella caerulea* (Gastropoda: Patellidae). *Zoology*, 1-11.
28. Plesch, B. (1977): An ultrastructural study of the musculature of the pond snail *Lymnaea stagnalis* (L.). *Cell Tissue Research* 180 (3), 317-340.

29. Ruyter, J. H. C. (1931): Eine einfache Methode für das Aufkleben von Zelloidin-Paraffinschnitten. Zeitschrift für wissenschaftliche Mikroskopie und für mikroskopische Technik 48, 226-227.
30. Sheehan, D. and Hrapchack, B. (1980): Theory and Practice of Histotechnology. St. Louis USA: Mosby, -481.
31. Shirbhate, R. and Cook, A. (1987): Pedal and opercular secretory glands of *Pomatias*, *Bithynia* and *Littorina*. Journal of Molluscan Studies 53, 79-96.
32. Smith, A. M. (1991): The role of suction in the adhesion of limpets. Journal of Experimental Biology 161, 151-169.
33. Smith, A. M. (1992): Alternations between attachment mechanisms by limpets in the field. Journal of Experimental Marine Biology and Ecology 160, 205-220.
34. Smith, A. M. (2002): The structure and function of adhesive gels from invertebrates. Integrative and Comparative Biology 42, 1164-1171.
35. Smith, A. M. (2006): Chapter: The biochemistry and mechanics of gastropod adhesive gels. In Smith, A. M. and Callow, J. A. (Eds.): *Biological Adhesives*. Heidelberg: Springer-Verlag, 167-182
36. Smith, A. M. (2010): Chapter: Gastropod secretory glands and adhesive gels. In von Byern, J. and Grunwald, I. (Eds.): *Biological Adhesive Systems: from Nature to Technical and Medical Application*. WienNewYork: Springer Verlag, 41-51
37. Smith, A. M., Quick, T. J., and St.Peter, R. L. (1999): Differences in the composition of adhesive and non-adhesive mucus from the limpet *Lottia limatula*. Biological Bulletin 196, 34-44.
38. Spicer, S. S. and Lillie, R. D. (1961): Histochemical identification of basic proteins with Biebrich Scarlet at alkaline pH. Stain Technology 6, 365-370.
39. Tonar, Z. and Markos, A. (2004): Microscopy and morphometry of integument of the foot of pulmonate gastropods *Arion rufus* and *Helix pomatia*. Acta Veterinaria Brno 73, 3-8.
40. Vijaya kumar, K., Kishore, B., and Hanumatha, R. K. (2013): Histology and histochemistry of the foot of *Lymnaea luteola* (Lamarck; 1799) Mollusca; Gastropoda. Journal of Experimental Biology and Agriculture Sciences 1 (2), 1-5.
41. von Byern, J., Scott, R., Griffiths, C., Micossi, A., and Cyran, N. (2011): Characterization of the adhesive areas in *Sepia tuberculata* (Mollusca, Cephalopoda). Journal of Morphology 272, 1245-1258.
42. Waite, J. H., Holten-Andersen, N., Jewhurst, S. A., and Sun, C. (2005): Mussel adhesion: Finding the tricks worth mimicking. The Journal of Adhesion 81 (3-4), 297-317.
43. Werneke, S. W., Swann, C. L., Farquharson, L. A., Hamilton, K. S., and Smith, A. M. (2007): The role of metals in molluscan adhesive gels. Journal of Experimental Biology 210, 2137-2145.

44. Wollesen, T., Cummins, S. F., Degnan, B. M., and Wanninger, A. (2010): FMRamide gene and peptide expression during central nervous system development of the cephalopod mollusk, *Idiosepius notoides*. *Evolution & Development* 12 (2), 113-130.
45. Wollesen, T., Loesel, R., and Wanninger, A. (2009): Pygmy squid and giant brains: mapping the complex cephalopod CNS by phalloidin staining of vibratome sections and whole-mount preparations. *Journal of Neuroscience Methods* 179 (1), 63-67.
46. Wondrak, G. (1967): Die exoepithelialen Schleimdrüsenzellen von *Arion empiricorum* (Fer.). *Zeitschrift für Zellforschung* 76, 287-294.
47. Wondrak, G. (2012): Monotypic gland-cell regions on the body surface of two species of *Arion*: Ultrastructure and lectin-binding properties. *Journal of Molluscan Studies* 78, 364-376.
48. Yamaguchi, K., Seo, N., and Furuta, E. (2000): Histochemical and Ultrastructural Analyses of the Epithelial Cells of the Body Surface Skin from the Terrestrial Slug, *Incilaria fruhstorferi*. *Zoological Science* 17 (8), 1137-1146.

8 ABBREVIATIONS

A1d - A5d, *Arion vulgaris* first, second, third, fourth, fifth dorsal gland type

At, *Arion vulgaris* transitional gland type

A1v - A4v, *Arion vulgaris* first, second, third, fourth ventral gland type

C1d - C4d, *Cepaea hortensis* first, second, third, fourth dorsal gland type

C1v - C2v, *Cepaea hortensis* first, second ventral gland type

ci, cilium

ep, epithelium

gt, gland type

H1d - H3d, *Helix pomatia* first, second, third dorsal gland type

H1v - H2v, *Helix pomatia* first, second ventral gland type

mi, microvilli

9 TABLES

Table 1: EDX elemental analyses of the *Arion vulgaris* mucus.

	Dorsal [atom %]	Ventral [atom %]
Carbon	51-57	19-47
Nitrogen	11-17	3-14
Oxygen	19-26	8-40
Sodium	0.2-1	1-2
Magnesium	0.1-0.5	0.2-1
Phosphorus	0.1-0.3	0.2-2
Sulfur	0.2-0.5	0.2-1
Chloride	1-7 as well as single values around 40	2-11 as well as measurements below 0.3
Potassium	2-8 as well as single data up to 44	4-14 as well as measurements below 1
Calcium	0.3-2	0.1-2

Table 2: EDX elemental analyses of *Helix pomatia* mucus.

	Dorsal [atom %]	Ventral [atom %]
Carbon	21-45	19-42
Nitrogen	3-12	1-4
Oxygen	11-40	3-59
Sodium	0.1-0.4	0,00
Magnesium	0.2-0.4	0.2-0.4
Phosphorus	0.1-1	0.1-0.3
Sulfur	0.5-1.5	0.1-0.3
Chloride	0.4-0.6 as well as single measurements up to 8-10	0.1-0.8
Potassium	2-14	0.2-5
Calcium	0.3-0.8 as well as single measurements up to 3-21	10-21 as well as measurements below 1

Table 3: EDX elemental analyses of the *Cepaea hortensis* mucus.

	Dorsal [atom %]	Ventral [atom %]
Carbon	20-34	24-47
Nitrogen	4-10	4-15
Oxygen	9-37	12-32
Sodium	0.6-1.5	0.5-3
Magnesium	0.1-0.3	0.2-0.7
Phosphorus	0,00	0.1-0.7
Sulfur	0.2-0.5	0.2-1.8
Chloride	8-27	6-16
Potassium	8-28	9-20
Calcium	0.2-0.3	0.2-1.8

Table 4: Summary of the gland characteristics

	<i>Arion vulgaris</i>									
Gland Name	A1d	A2d	A3d	A4d	A5d	At	A1v	A2v	A3v	A4v
Location	dorsal	dorsal	dorsal	dorsal	dorsal	big groove	ventral	ventral	ventral	ventral
Histochemistry glands										
PAS	-	-	-	-	-	xx	r++	r++	r++	-
Toluidine blue O pH 4.3	r++	r++	-	r++	r++	xx	r++	r++	r++	-
Alcian blue pH 1.0	r+-	r+-	-	-	r+-	xx	r++	r++	r++	-
Alcian blue pH 2.5	r++	r++	-	r++	r++	xx	r++	r++	r++	-
Safranin-O	-	-	-	-	-	xx	r++	r++	r++	-
Biebrich Scarlet pH 6.0	-	-	-	-	-	xx	-	-	-	-
Biebrich Scarlet pH 8.0	-	-	-	-	-	xx	-	-	-	-
Biebrich Scarlet pH 9.5	-	-	-	-	-	xx	-	-	-	-
Biebrich Scarlet pH 10.5	-	-	-	-	-	xx	-	-	-	-
Calcium	-	-	-	-	-	xx	-	-	-	+
DOPA	-	-	-	-	-	xx	-	-	-	-
Lectin binding in tissue										
ConA	-	-	-	-	-	xx	-	-	-	-
PNA	-	-	-	-	-	xx	-	-	-	-
SBA	-	-	-	-	-	xx	-	-	-	-
WGA	-	-	-	-	-	xx	-	-	-	-
GNA	-	-	-	-	-	xx	-	-	-	-
UEA	-	-	-	-	-	xx	r++	r++	r++	-
Histochemistry secreted mucus										
	dorsal mucus						ventral mucus			
Calcium	++					n.d.	++			
Sudan Black B (lipids)	+					n.d.	++			
Elements										
	dorsal mucus [atom%]						ventral mucus [atom%]			
Carbon	51 - 57					n.d.	19 - 47			
Nitrogen	11 - 17					n.d.	3 - 14			
Oxygen	19 - 26					n.d.	8 - 40			
Sodium	0.2 - 1					n.d.	1 - 2			
Magnesium	0.1 - 0.5					n.d.	0.2 - 1			
Phosphorus	0.1 - 0.3					n.d.	0.2 - 2			
Sulfur	0.2 - 0.5					n.d.	0.2 - 1			
Chlorine	1 - 7 % and single values > 40 %					n.d.	2 - 11 % and values < 0.3 %			
Potassium	2 - 8 % and single values > 44 %					n.d.	4 - 14 % and values < 1 %			
Calcium	0.3 - 2					n.d.	0.1 - 2			

strong positive	++
positive	+
weak positive	+-
no reaction	-
at least one gland reactive	r
not visible	xx
not determined	n.d.

<i>Helix pomatia</i>					<i>Cepaea hortensis</i>					
H1d	H2d	H3d	H1v	H2v	C1d	C2d	C3d	C4d	C1v	C2v
dorsal	dorsal	dorsal	ventral	ventral	dorsal	dorsal	dorsal	dorsal	ventral	ventral
-	++	-	r++	r++	++	r++	r++	-	+-	r+-
++	++	-	r++	r++	++	r++	r++	-	++	r++
++	++	-	r++	r++	++	r++	r++	-	++	r++
++	++	-	r++	r++	++	r++	r++	-	++	r++
+	++	-	r++	r++	++	+-	+-	-	+-	r+-
-	-	-	-	-	-	-	-	-	-	-
-	-	-	-	-	-	r++	r++	-	-	-
-	-	-	-	-	-	-	-	-	-	-
-	-	-	-	-	-	-	-	-	-	-
-	-	-	-	-	-	-	-	-	-	-
-	-	-	-	-	-	-	-	-	-	-
-	-	-	-	-	-	-	-	-	-	-
-	-	-	-	-	-	-	-	-	-	-
-	-	-	-	-	r+	r+	r+	-	-	-
-	-	-	-	-	-	-	-	-	-	-
-	-	-	-	-	-	-	-	-	-	-
-	-	-	-	-	r+	r+	r+	-	-	-
-	+	-	r++	r++	-	r++	r++	-	r+	r+
-	+	-	r++	r++	r+	r+	r+	-	-	-
dorsal mucus		ventral mucus			dorsal mucus		ventral mucus			
+		+-			+-		+-			
+		++			+		+-			
dorsal mucus [atom%]		ventral mucus [atom%]			dorsal mucus [atom%]		ventral mucus [atom%]			
21 - 45		19 - 42			20 - 34		24 - 47			
3 - 12		1 - 4			4 - 10		4 - 15			
11 - 40		3 - 59			9 - 37		12 - 32			
0.1 - 0.4		0.0			0.6 - 1.5		0.5 - 3			
0.2 - 0.4		0.2 - 0.4			0.1 - 0.3		0.2 - 0.7			
0.1 - 1		0.1 - 0.3			0.0		0.1 - 0.7			
0.5 - 1.5		0.1 - 0.3			0.2 - 0.5		0.2 - 1.8			
0.4 - 0.6 % and values > 8 - 10 %		0.1 - 0.8			8 - 27		6 - 16			
2 - 14		0.2 - 5			8 - 28		9 - 20			
0.3 - 0.8 % and values > 3 - 21 %		10 - 21 % and values < 1 %			0.2 - 0.3		0.2 - 1.8			

10 FIGURE LEGENDS

Arion vulgaris

Figure 1: Schematic overview of the distribution pattern of the gland cells of *Arion vulgaris*. It becomes evident that in the dorsal area the gland type A4d is rare, while others like A1d or A3d are more common. In the ventral region the gland types A1v, A2v and A3v are frequently present, although A3v does not appear as numerous as the others. A4v in contrast only occurs in the border area, where cilia are missing. The gland type At occurs only in the transition region. Also a noticeable difference in the distribution of the cilium border in the different regions of *Arion vulgaris* is disclosed. Dorsally a microvilli layer (mv) covers the epithelium (ep), while in the ventral area beside the microvilli layer also a cilia border (ci) is given. The arrow marks the point, where the cilia emerge in the big groove. Scale bars: 250µm (A); 1µm (A2d, A4d, A1v, A2v); 0.5µm (A1d, A3d, A5d, A3v, A4v, At).

Figure 2: Schematic overview of the subepidermal gland types in the dorsal and ventral pedal integument of *Arion vulgaris*. **A**, in the dorsal region of the foot five gland types could be differentiated, labeled as A1d, A2d, A3d, A4d and A5d. In the transition region one gland type appears (At (insert)). **B**, in the ventral region four gland types (A1v, A2v, A3v and A4v) could be observed. Scale bars: 50µm (A & B).

Figure 3: Morphological appearance of the different gland types in the dorsal and ventral region of the foot of *Arion vulgaris* (semithin-sectioning, Toluidine blue staining). **A**, the gland types A1d, A3d, and A5d could be observed, which greatly differ by their secretory material. **B**, several glands of the type At are located in the same area; only at the ventral region cilia can be observed (asterisk). **C**, the gland types A1d, A3d and A4d are located next to each other and likewise the difference in the secretory material is obvious. **D**, the gland type A4v contains fine granulated material and occurs in the border region of the ventral side. **E**, the granules of the gland type A2d have a small globular shape; **F**; in the ventral area three gland types are common; distinguishable by the appearance of their granules. **A, E & F**, cell nuclei are visible inside the gland cells (arrowheads). Scale bars: 25µm (A, D, E, F); 10µm (B, C).

Figure 4: Content of the different gland types in the dorsal and ventral pedal integument of *Arion vulgaris* (transmission electron microscopy).

A, the difference of the granules between A1d and A3d is clearly visible; the cell nuclei of A3d is prominent (arrowhead); A1d extrudes the granules in whole packages (insert). **B**, the granules of A4d have nearly the same size as that of A1d, but they have a rounded shape instead of the elongated one of A1d. **C & D**, the content of A2d and A5d is fine granulated material; in A2d round granules of a bigger size (small arrowheads) are observed too, which are not visible in A5d; the potential formation area of the granulated material in A5d is visible (big arrowhead). **E**, At only appears in the transition zone; shortly before the release of the granules a transformation occurs; the cilia roots are visible (arrowheads); the cross section demonstrates the presence of the cilium border at this area (insert). **F**, the granulated material of A4v is not packed very dense. **G**, in the ventral region three different gland types (A1v, A2v and A3v) can be observed, all appearing in high abundance. Scale bars: 2.5 μ m (A, C, D, E, G); 2 μ m (A-insert, B); 0.5 μ m (E-insert, F).

Figure 5: Content of the different gland types in the dorsal and ventral pedal integument of *Arion vulgaris* (scanning electron microscopy).

A, in this region of the foot three gland types could be differentiated and according to their content they are assigned to the gland types A1d, A3d and A4d. **B**, the granules of gland type A3d are globular and the smallest of all three glands. **C**, the granules of gland type A1d are elongated. **D**, the content of gland type A4d are globular granules as well, but they are much bigger than that of gland type A3d. **E**, in the ventral region one gland type could be observed, marked with gt. **F**, the observed granules are globular and always a few of them stick together. Scale bars: 10 μ m (A, E); 5 μ m (B, C, D, F).

Figure 6: Applied histochemical staining of the dorsal pedal integument of *Arion vulgaris*.

A, with Periodic acid-Schiff reaction (PAS) only the connective tissue but not the secretory material of the gland types is stained (arrowheads). **B**, Toluidine blue staining, gamma metachromasia in one or more of the larger glands is visible (gt). **C**, Alcian blue staining (pH level 1.0) as well as **D**, Alcian blue staining (pH level 2.5), showing that one or more of the bigger gland types (gt) as well as their ducts (arrowheads) are stained (gt) positively. **E**, Azan staining; muscle strands are clearly visible (arrowheads); large cavities are visible next to the gland cells in the subepithelial tissue (rhombus). **F**, Safranin-O staining, the secretory material of the large gland types shows no histochemical reaction (gt). **A-F**, gland

type A3d with some deposits is visible under the surface (asterisks). **A-D**, a pigmentation of the tissue is noted (arrows). **B, E & F**, cell nuclei are visible in the epithelium (arrowheads). Scale bars: 100 μ m (A-F).

Figure 7: Applied histochemical stainings of the ventral pedal integument of *Arion vulgaris*. **A**, Periodic acid-Schiff reaction (PAS), one or more of the ventral gland types is colored in dark pink (arrowheads). **B**, Toluidine blue staining, gamma metachromasia in one or more glands is visible (arrowheads). **C**, Alcian blue staining (pH level 1.0) as well as **D**, Alcian blue staining (pH level 2.5), positive staining of one or more gland types is noted (arrowheads). **E**, Azan staining; muscle strands are clearly pictured (arrows); cell nuclei are visible in the epidermis (arrowheads). **F**, Safranin-O staining, one or more of the glands is stained in dark red (arrowheads). **G**, Alizarin red S staining, positive stained deposits in the superepithelial layer visible (arrowheads). **H**, Sudan black B staining, positive lipid staining in the mucus is observed. **A, C & D**, a pigmentation of the tissue is noted (arrow). Scale bars: 100 μ m (A-H).

Figure 8: Positive lectin signals in the ventral pedal integument (A) and muscle reconstructions (phalloidin C & D), as well as the distribution pattern of one gland type, in the dorsal pedal integument (μ -CT E & F) (confocal laser scanning microscopy & μ -CT). **A**, the secretory material of one or more gland types shows a strong affinity for α -L-fucose (lectin UEA) (arrows); **glowing / illumination** of the epithelium results from autofluorescence (arrowhead). **B**, the secreted mucus shows the same affinity for α -L-fucose (lectin UEA). **C&D** subepidermal dorsal cells (not visible) enclosed by the muscle fiber network (arrowheads); cell nuclei are visible (arrow). **E**, distribution pattern of one of the dorsal gland types (arrows). **F**, dorsal integument with the stained content of one gland type (arrow). Scale bars: 50 μ m (B); 25 μ m (C).

Figure 9: Elemental analysis of the dorsal and ventral secretory material (energy dispersive X-ray analysis). **A**, SEM analyses indicate the presence of crystals in the dorsal mucus, which **B**, appears to consist of chloride. **C**, also the element potassium is uniformly distributed in the dorsal mucus (arrow). **D**, in the ventral mucus likewise crystals could be observed. **E**, the element chloride is not uniformly distributed but appears patched **F**, the element potassium is present in high abundance (arrow). Scale bars: 50 μ m (A&D); 20 μ m (B, C, E&F).

Helix pomatia

Figure 10: Schematic overview of the distribution pattern of the gland cells of *Helix pomatia*.

All gland types in the dorsal area (H1d, H2d, H3d) are very common, but H3d occur more often than the other ones. In the ventral area H1v appears in large numbers, while H2v is less abundant. The cilium border is on the ventral side of the foot, in the same region where H1d, H2d and H3d disappear and become elongated in the middle of the ventral side. Dorsally a microvilli layer (mv) covers the epithelium (ep), while in the ventral area beside the microvilli layer also a cilia border (ci) is given. Scale bars: 250µm (A); 1µm (H1d, H2d, H3d, H1v, H2v).

Figure 11: Schematic overview of the dorsal and ventral pedal gland types of *Helix pomatia*. **A**, in the dorsal region of the foot three gland types are given, marked with H1d, H2d and H3d. For the gland type H2d two types of secretory material could be observed, marked as H2d and H2d*. **B**, two gland types, marked with H1v and H2v, are visible in the ventral region of the foot. Scale bars: 50µm (A&B).

Figure 12: Morphological appearance of the different gland types in the dorsal and ventral region of the foot of *Helix pomatia* (semithin-sectioning, Toluidine blue staining). **A**, the dorsal gland types H1d, H2d and H3d are differentiated by their shape and content. **B & C**, H1v is in the ventral pedal region. **D**, The 'open' distal cell poles indicate active secretion of the gland types H1d and H3d. **E**, areas of clumped secretory granules in H1v, shortly before secretion takes place (asterisk). **F**, the granules of H1v and H2v have a spherical shape, whereby they are of a high density in H1v but almost electron lucent in H2v. Scale bars: 20µm (A, B, D, F); 10µm (C&E).

Figure 13: Content of the different gland types in the dorsal and ventral pedal integument of *Helix pomatia* (transmission electron microscopy). **A**, two different gland types (H2d, H3d) in the dorsal region could be observed with differ clearly in the morphology of their secretory content by e.g. **B**, having 'ice floes'-like granules (given for gland type H1d). **C**, In the case of gland type H2d/H2d* it remains unclear if there are different synthesis stages of the granulated material or two distinct gland types. **D**, the gland type H1v with its granulated secretory material in the process of secretion ; arrowhead marks the cell

membrane. **E and F**, Comparison of H1v and H2v pointing out the structural difference of the granules; arrowheads mark the nuclei. Scale bars: 2 μ m (A-F).

Figure 14: Dorsal and ventral gland types of *Helix pomatia* (scanning electron microscopy). **A, B & C** in the dorsal area of *Helix pomatia* gland types (H1d, H2d, H3d) of variable sizes and content are visible. **D**, in the ventral pedal integument a gland type with spherical granules of different sizes can be observed. This gland cannot be assigned to one of the histochemically characterized gland types so far. **E**, the granules of the gland type H2d have a spherical shape. Scale bars: 10 μ m (A, C - E); 2.5 μ m (B).

Figure 15: Applied histochemical stainings of the dorsal pedal integument of *Helix pomatia*. **A**, Periodic acid-Schiff reaction (PAS); a strong positive staining of the secretory material is apparent in gland type H2d, while the mucus of H1d is negative for sugars (right picture). **B**, Toluidine blue staining causes gamma metachromasia in H2d (left picture) and H1d (right picture). **C**, Alcian blue staining (pH level 1.0) as well as **D**, Alcian blue staining (pH level 2.5) shows a strong positive coloring of H1d and H2d (arrowheads). **E**, PAS - Alcian blue combination staining (pH level 1.0) as well as **F**, PAS - Alcian blue combination staining (pH level 2.5) showing only a reaction to Alcian blue staining in H1d; a staining of PAS and Alcian blue in H2d. **G**, Alizarin red S staining points out a strong reaction around the cell wall of H1d. **H**, Safranin-O staining; both gland types are positively stained in light red. **B&G**, cell nuclei are visible in the epithelium (arrow). Scale bars: 100 μ m (C - H); 50 (A&B).

Figure 16: Applied histochemical stainings of the ventral pedal integument of *Helix pomatia*. **A**, Periodic acid-Schiff reaction (PAS) leads to a dark pink coloration of the glands (arrowheads). **B**, Toluidine blue staining provokes gamma metachromasia in some glands (arrowheads). **C**, Alcian blue staining (pH level 1.0) as well as **D**, Alcian blue staining (pH level 2.5) effects a positive reaction of one or both gland types (arrowheads). **E**, Azan staining; muscle strands are clearly pictured (arrowheads). **F**, Safranin-O staining, a gland type stained in dark red is visible (arrowheads). **G**, positive reaction of the ventral mucus with Sudan black B visible. Scale bars: 100 μ m (A - F); 50 μ m (G).

Figure 17: Lectin signals and muscle reconstructions in the pedal integument (confocal laser scanning microscopy). **A**, gland type H2d shows a strong affinity for mannose (lectin GNA, arrowheads) as well as **B**, for α -L-fucose (lectin UEA, arrows) in the dorsal pedal

surface. **C**, Phalloidin staining illustrating the muscle network of the foot. **D**, gland type H1v shows a strong affinity for mannose (lectin GNA) and **E**, for α -L-fucose (lectin UEA) in the ventral pedal surface (arrows). **B**, **D** & **E**, staining of the epithelium results from autofluorescence (arrowhead). Scale bars: 100 μ m (D&E); 50 μ m (B).

Figure 18: Elemental analysis of the dorsal and ventral secretory material (energy dispersive X-ray analysis). **A**, Imaging of the mucus indicate the presence of crystals in the dorsal mucus, which **B**, consists among others also of potassium. **C**, Also sulphur could be detected in different regions (arrow). **D**, Also in the ventral mucus a crystallisation of some elements as i.e. **E**, potassium occurs. **F**, Again sulphur is irregular distributed in the isolated mucus (arrow). Scale bars: 50 μ m (A&D); 20 μ m (B, C, E&F).

Cepaea hortensis

Figure 19: Schematic overview of the distribution pattern of the gland cells of *Cepaea hortensis*.

In the dorsal area the gland types C1d and C4d are the common distributed, while the gland types C2d and C3d are rarely observed. In contrast in the ventral area only one gland type (C1v) is frequently present, while another one (C2v) could only be found sporadically. Beside the number of gland types, the ventral foot area is covered, aside from the microvilli layer (mi), by an cilium border (ci) which could not be observed in the dorsal region. The inserts show the granules of each gland type, as well as the deposits found in the ventral epithelium. Scale bars: 250 μ m (A); 1 μ m (C2d, C3d, C4d, deposit inserts); 0.5 μ m (C1d, C2v inserts); 0.25 μ m (C1v inserts).

Figure 20: Schematic overview of the dorsal and ventral pedal integument of *Cepaea hortensis*. **A**, In the dorsal region of the foot four gland types (named C1d, C2d, C3d and C4d) could be differentiated according to their shape and secretory content. **B**, two gland types, dedicated as C1v and C2v are traversing the connective and epithelial layers of the ventral foot. Here a cilium border (ci) is visible, while in the dorsal area only microvilli (mi) could be found. Furthermore an epithelial cell type (ep) with dark granular deposits could be observed. Scale bars: 50 μ m (A & B)

Figure 21: Characterization of the different gland types in the dorsal and ventral region on semithin level. **A**, Gland cells C2d and C3d of the dorsal epithelium bear an almost similar granular content, while the material of gland type C1d clearly differs by having the ice-floes pattern. **B**, the content of the gland type C4d is very finely granulated. **C**, detailed view of the ice-floes-patterned secretory material of C1d and secreted content (arrowhead). **D**, In the ventral region two gland types are present: C1v with small granules (asterisk and insert f) and C2d (insert e) with flocculent material. Scale bars: 25 μ m (A - D); 5 μ m (inserts).

Figure 22: Content of the different gland types in the dorsal and ventral pedal integument of *Cepaea hortensis* in TEM.

A, Secretion opening of C1d through the microvilli layer. **B** the granules of C2d contain mostly electron-dense spots and an electron-lucent outer layer. **C**, the secretory material of C4d consists of very fine, uniform material. **D**, the granules of the ventral gland type C1v have an almost spherical shape and they merge in the apical area near the secretory opening. **E**, the granules of C2v are densely packed in relation to those of C1v; some deposits are observed in the neighbored epithelial glands (arrowheads). **F**, C1d and C2d lying next to each other; here it is clearly visible that the granules of C1d are a lot bigger and have a grainy texture, while the ones of C2d appear mostly homogeneous. **G**, the granules of C3d are slightly polygonal, appear electron-dense and contain homogeneous material. **H**, the granules in C2v as for C1v also the granules of C2v merge in the apical area before release. **I**, cross section of two cilia of the ventral foot epithelium, showing the typical 9x2 + 2 microtubule pattern. Scale bars: 2 μ m (A - H); 0.25 μ m (I).

Figure 23: SEM characterization of the secretory content in the different gland types of *Cepaea hortensis*. **A**, in the dorsal epithelium spherical granules of different diameter ($\approx 0.2\mu$ m - $\approx 1\mu$ m) could be observed in a gland type (gt). However, a dedication of this secretory content to gland types C2d or C3d is not possible at this stage. **B**, the granules of C1d with their ice-float appearance. **C, D & E**, also in the ventral pedal integument spherical granules could be observed; however, the granules appear slightly larger ($\approx 1\mu$ m - $\approx 2.2\mu$ m) than those dorsally. As for the dorsal epithelium, also the ventral gland types cannot be correlated to one of the two gland types (C1v, C2v). Scale bars: 20 μ m (B); 5 μ m (A, D&E); 2.5 μ m (C).

Figure 24: Histochemical stainings of the dorsal pedal integument. The gland type C1d as well as the gland type Cd2 or Cd3 stains positive for **A**, Periodic acid-Schiff (PAS) **B**, for

Toluidine blue staining **C**, for Alcian blue staining (pH level 1.0) as well as **D**, Alcian blue staining (pH level 2.5) **E**, with Azan staining a fourth gland type (C4d) with fine content is visible. Empty cavities (rectangles) within the subepithelial tissue are visible, however, it need to be verified why the secretory material did not become stained. **F**, The secretory material of Cd1 stains strongly positive for mucin (red coloration) while the material of C4d did not show a reaction to Safranin-O and remains stained bluish green. **B, D & F**, cell nuclei in the epithelial layer (arrowheads). **C&D**, mucus secretion is shown (in C arrow). Scale bars: 100µm (A - F); 25µm (inserts).

Figure 25: Histochemical stainings of the ventral pedal integument. The glandular material of C1v reacts strongly for **A**, sugars (Periodic acid-Schiff reaction) **B**, for acidic proteins (Toluidine blue staining) (C1v pentagon). **C**, acidic proteins (Alcian blue at pH level 1.0) (C1v asterisks) as well as **D**, at Alcian blue (pH level 2.5) (C1v asterisks). **E**, Azan staining shows the dense dermal muscle net (arrows). **F**, the secretory material of C1v stains positive with Safranin-O for mucin (asterisks). **B & D**, cell nuclei point out the epithelial layer (arrowheads). Scale bars: 100µm (A - F).

Figure 26: Further histochemical staining of the gland types A, with Biebrich scarlet (pH 8.5) the gland type C2d or C3d as well as the cell nuclei (arrowhead) becomes stained **B**, Alizarin red S indicates that calcium is present not only in the secretory material of C1d but in particular in the gland surrounding. **C**, the secreted mucus from the ventral foot area stains positive for lipids (black dots) by Sudan black B. **D**, The secretory material of C1v stains positive for acidic proteins only (Alcian blue at pH level 2.5) **E**, the deposit in the epithelial cells likewise stains for basic proteins (Biebrich Scarlet at pH level 8.5) as the secretory material C2d/C3d gland type in the dorsal epithelium (Fig. 23A). Scale bars: 100µm (B); 50µm (D); 25µm (A, C, E).

Figure 27: Lectin reaction (A, B and D) and muscle reconstructions (C and E) of the pedal integument (confocal laser scanning microscopy). **A & B**, granules of gland type C2d/C3d as well as the epithelium surface show a strong affinity to mannose (lectin GNA) in the dorsal pedal surface (arrowheads). **C&E** muscle fibre net on the dorsal region of the foot, transverse muscle strands can be seen (arrowheads)(actin-staining with phalloidin, CLSM). **D**, as for the dorsal pedal area, mannose (lectin GNA) is also present in glands (arrowheads) of

the ventral pedal surface.. **A, B & D**, staining of the epithelium results from autofluorescence (arrow). Scale bars: 50µm (C, D); 25µm (A&E).

Figure 28: Elemental analysis of the dorsal and ventral secretory material (energy dispersive X-ray analysis). **A**, SEM image of the dried dorsal mucus shows sign of element crystallisation as for example given for **B**, chlorine **C**, and potassium (arrow). **D**, Also ventrally crystals containing of **E**, chlorine or **F**, potassium is contained in the sample (arrow). Scale bars: 50µm (A&D); 20µm (B, C, E&F).

11 FIGURES *Arion vulgaris*

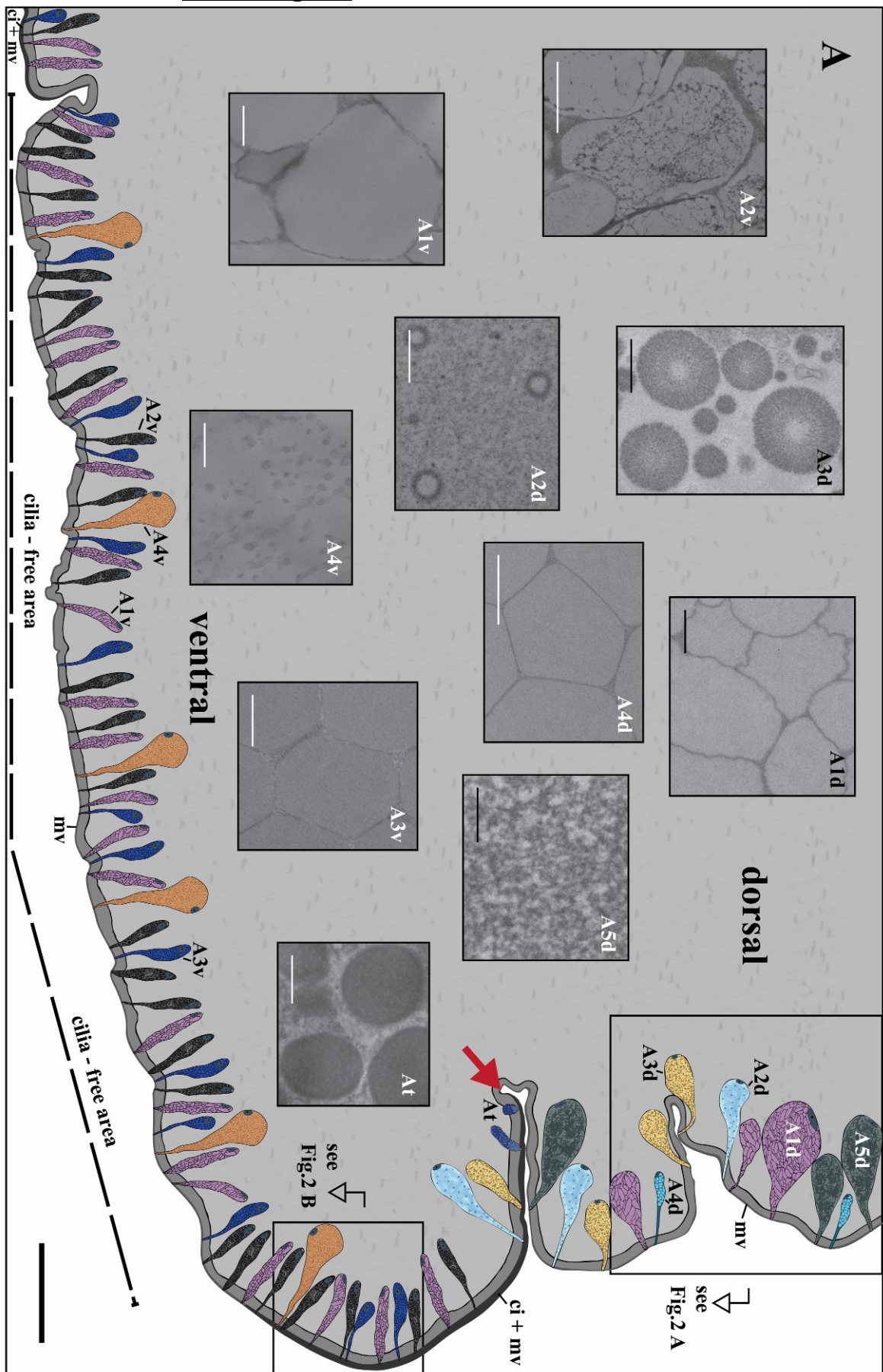


Figure 1

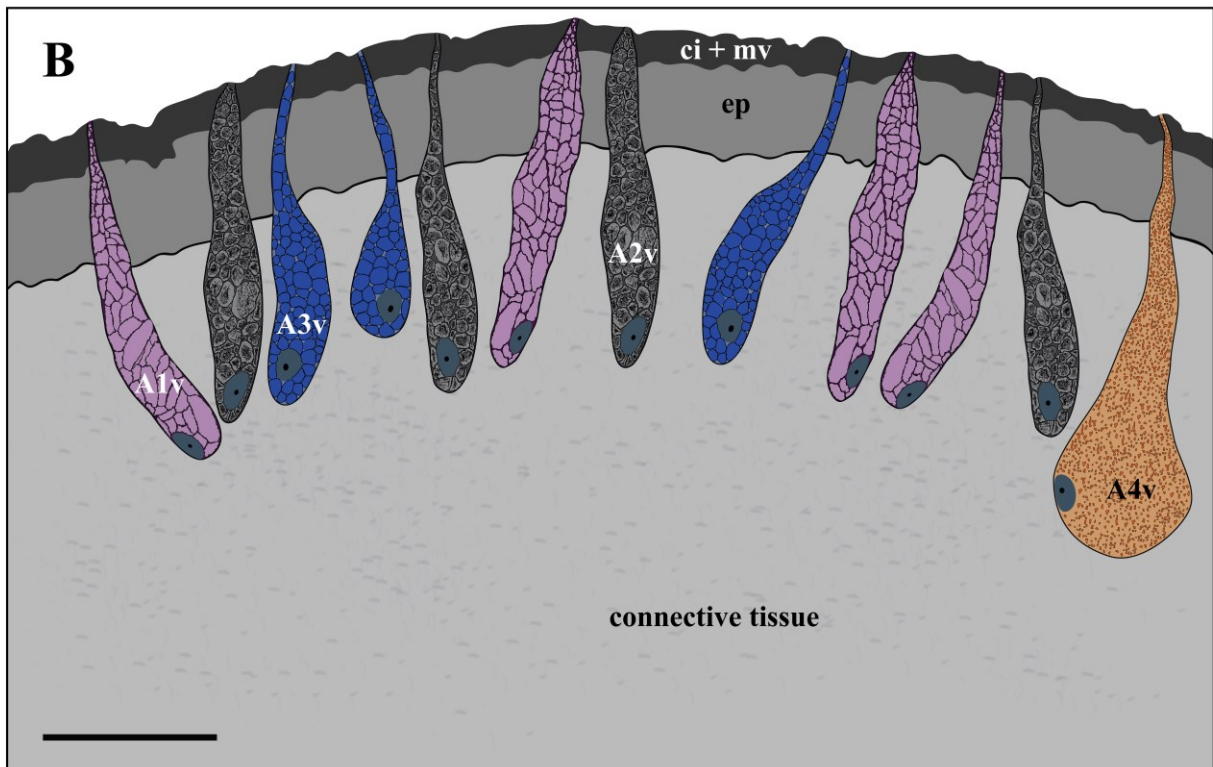
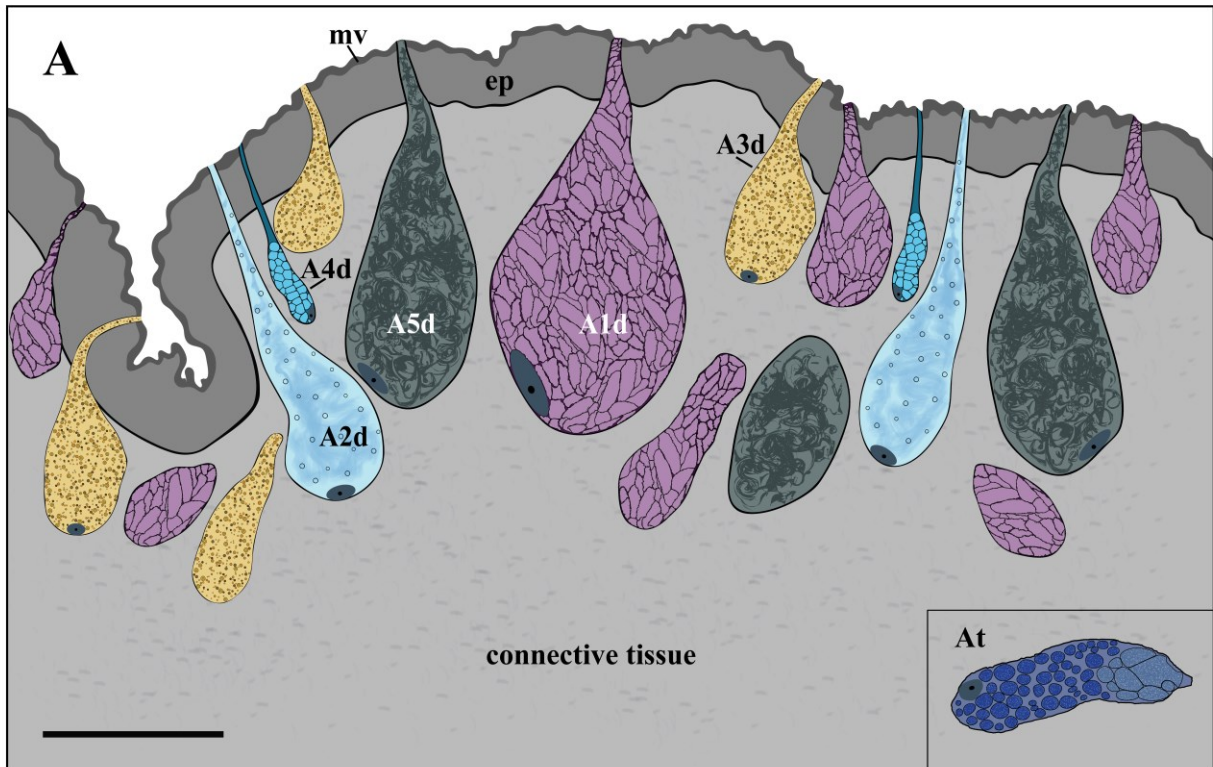


Figure 2

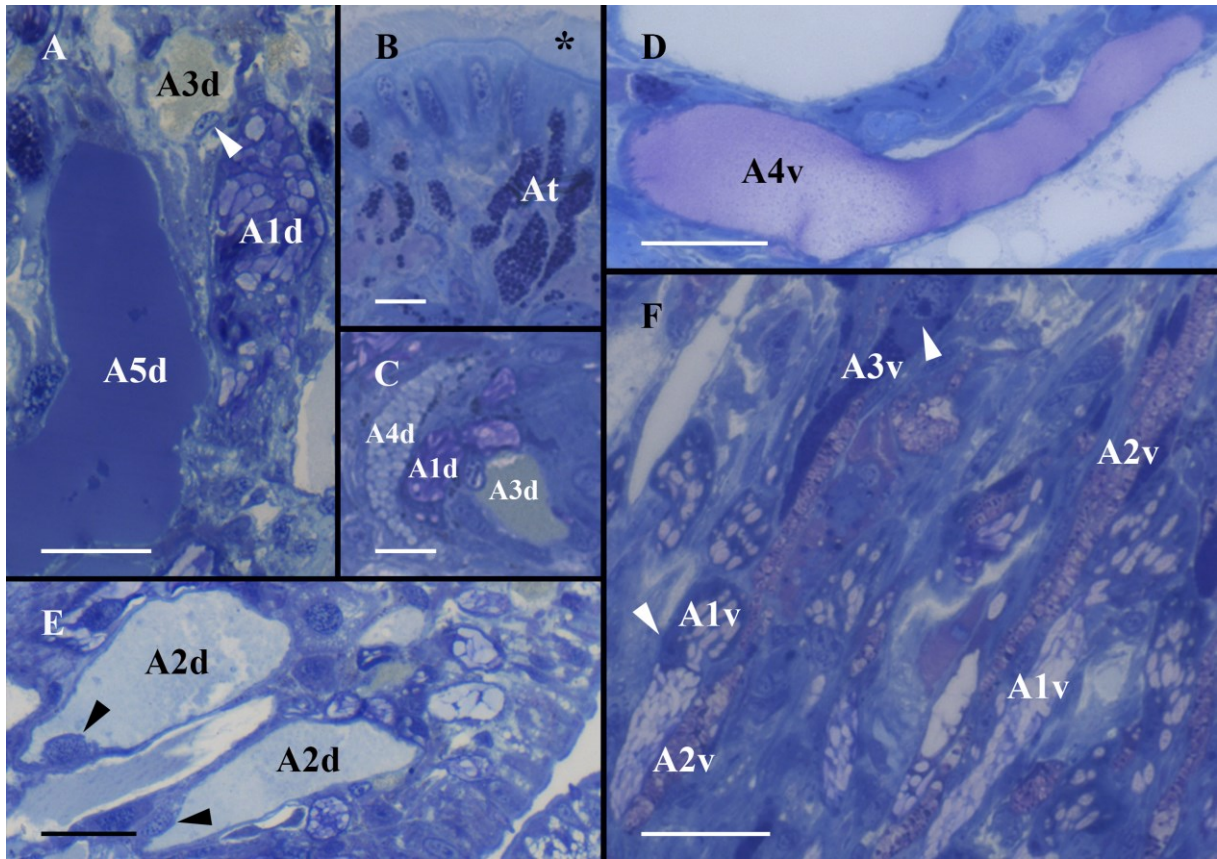


Figure 3

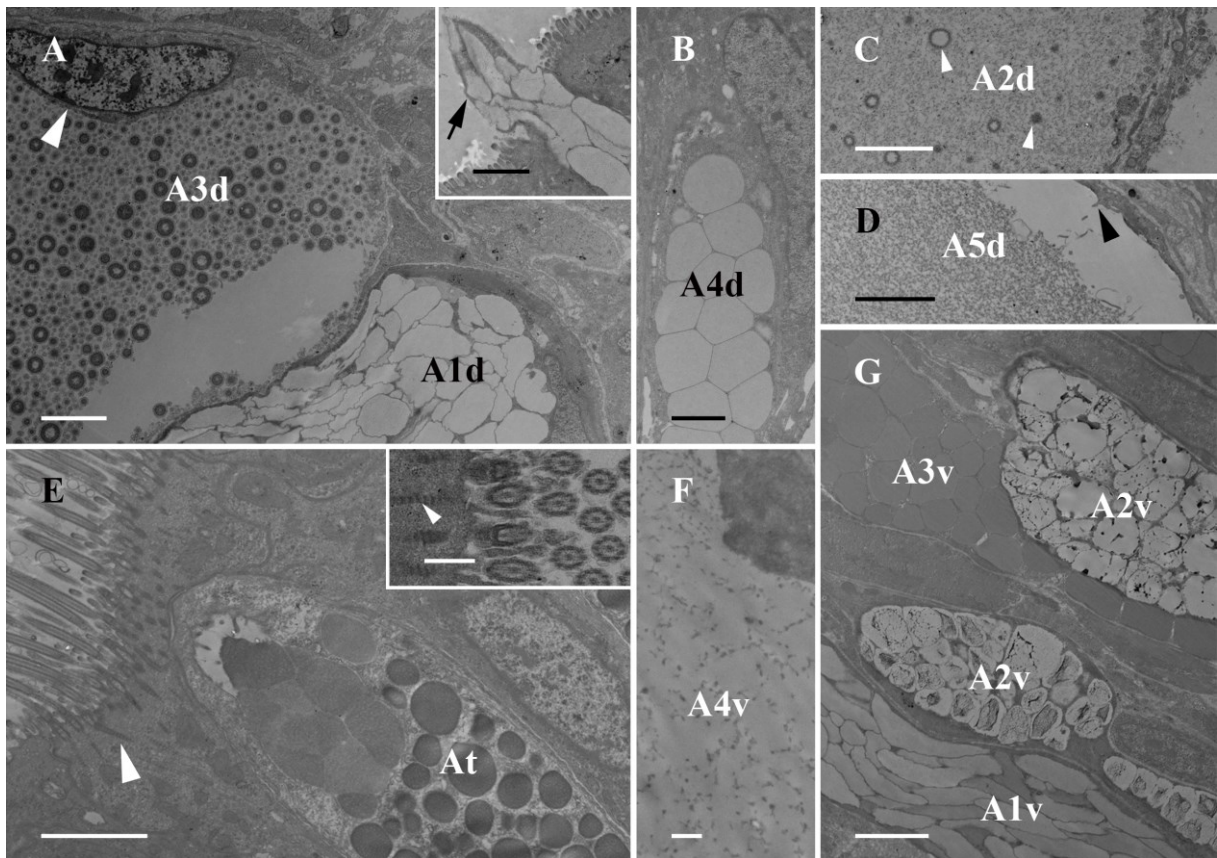


Figure 4

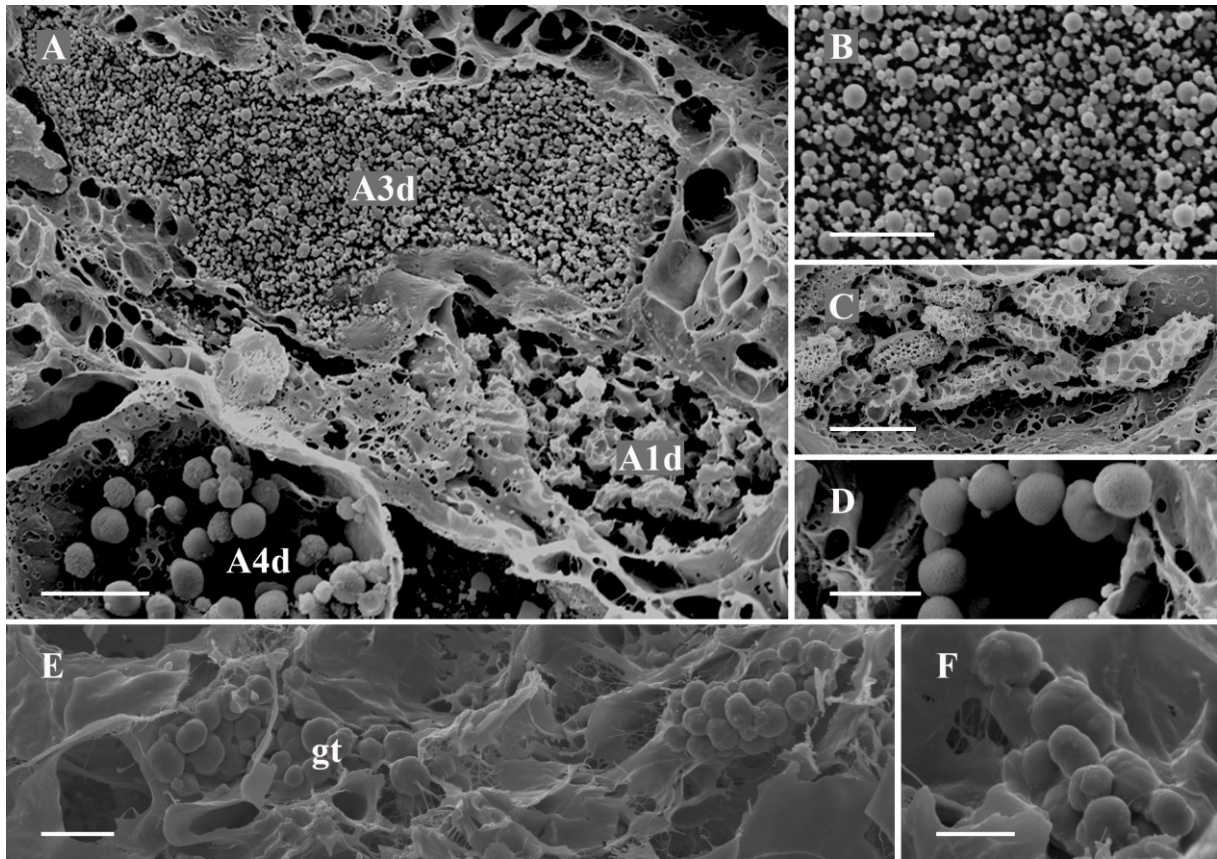


Figure 5

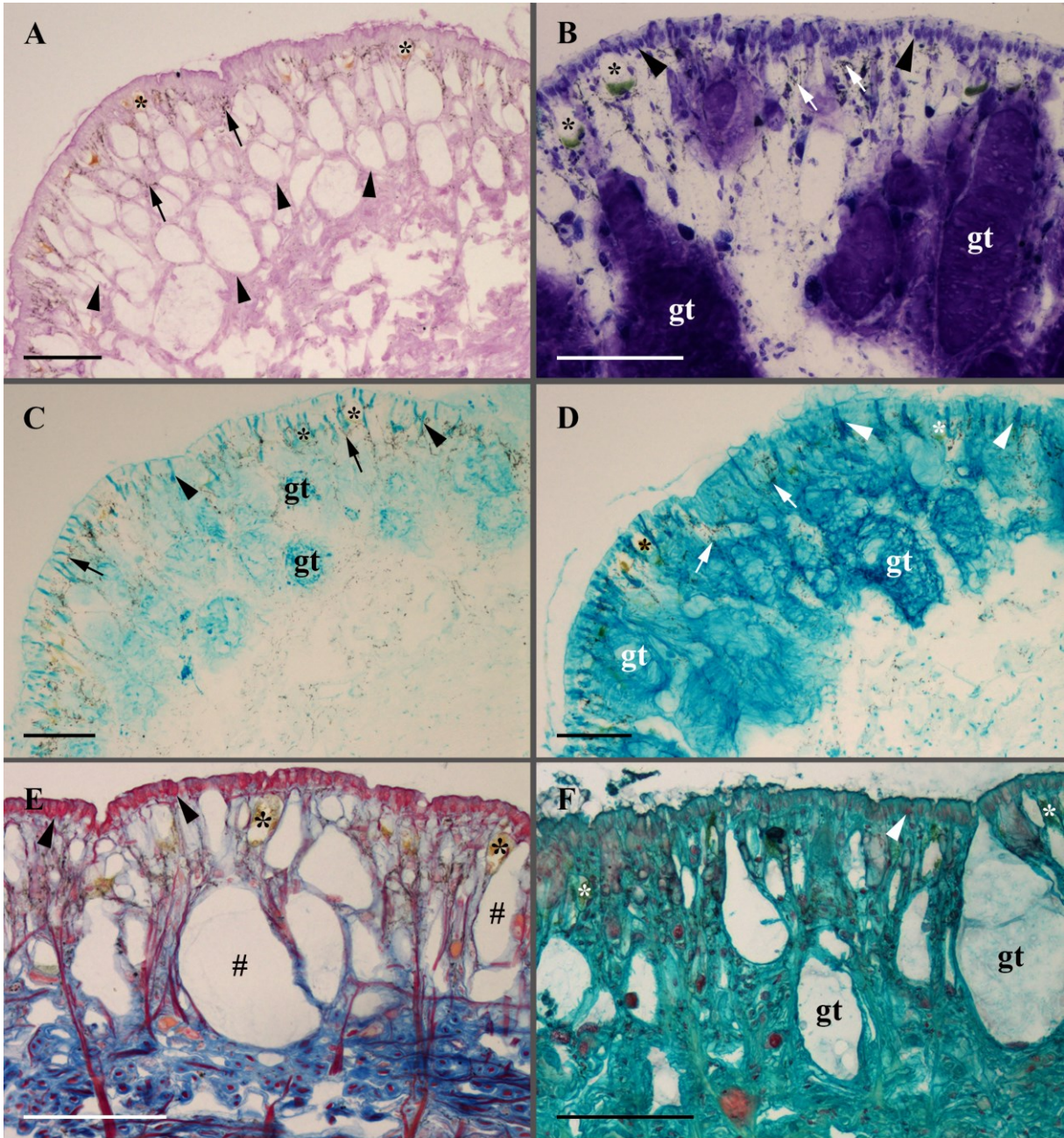


Figure 6

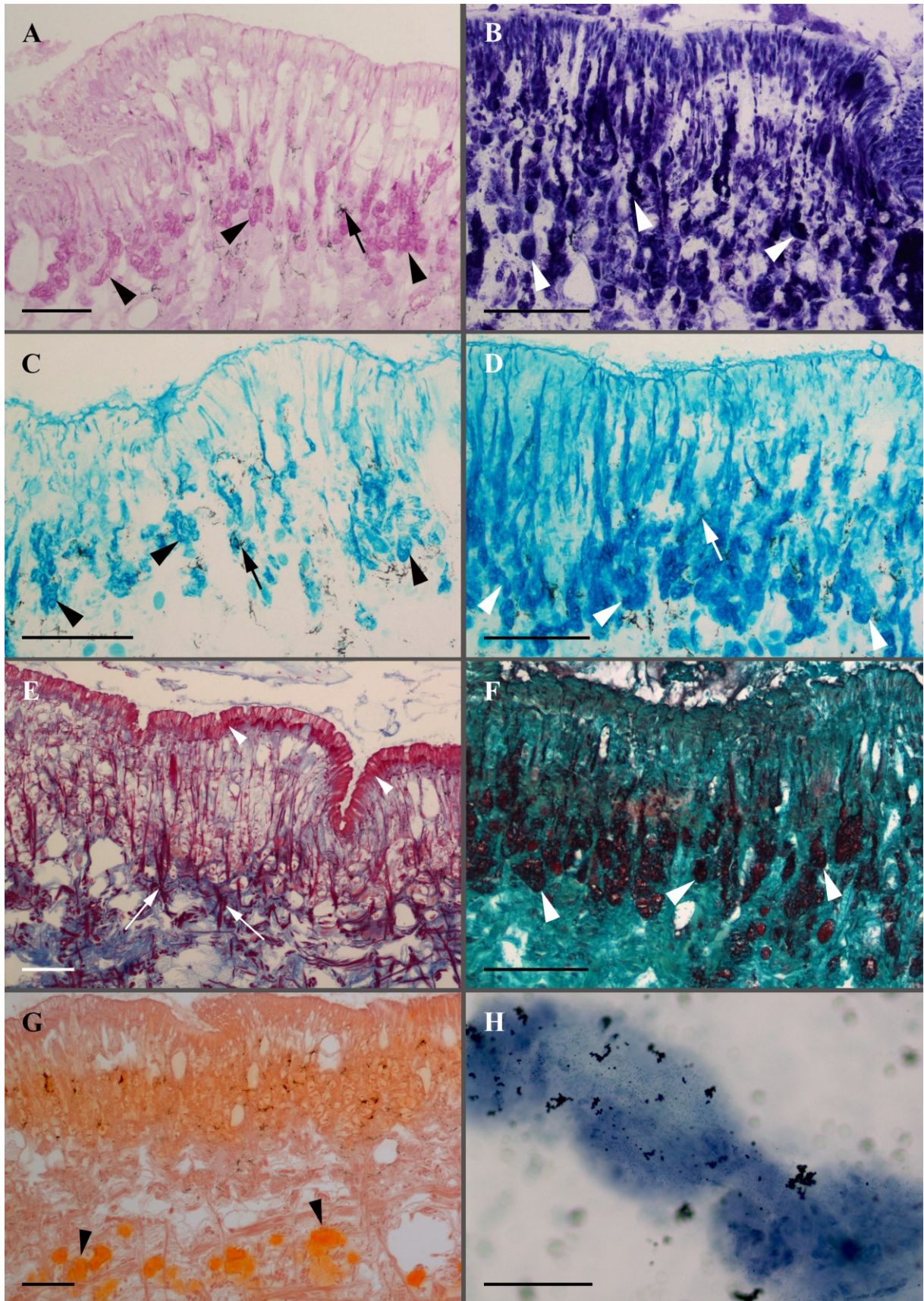


Figure 7

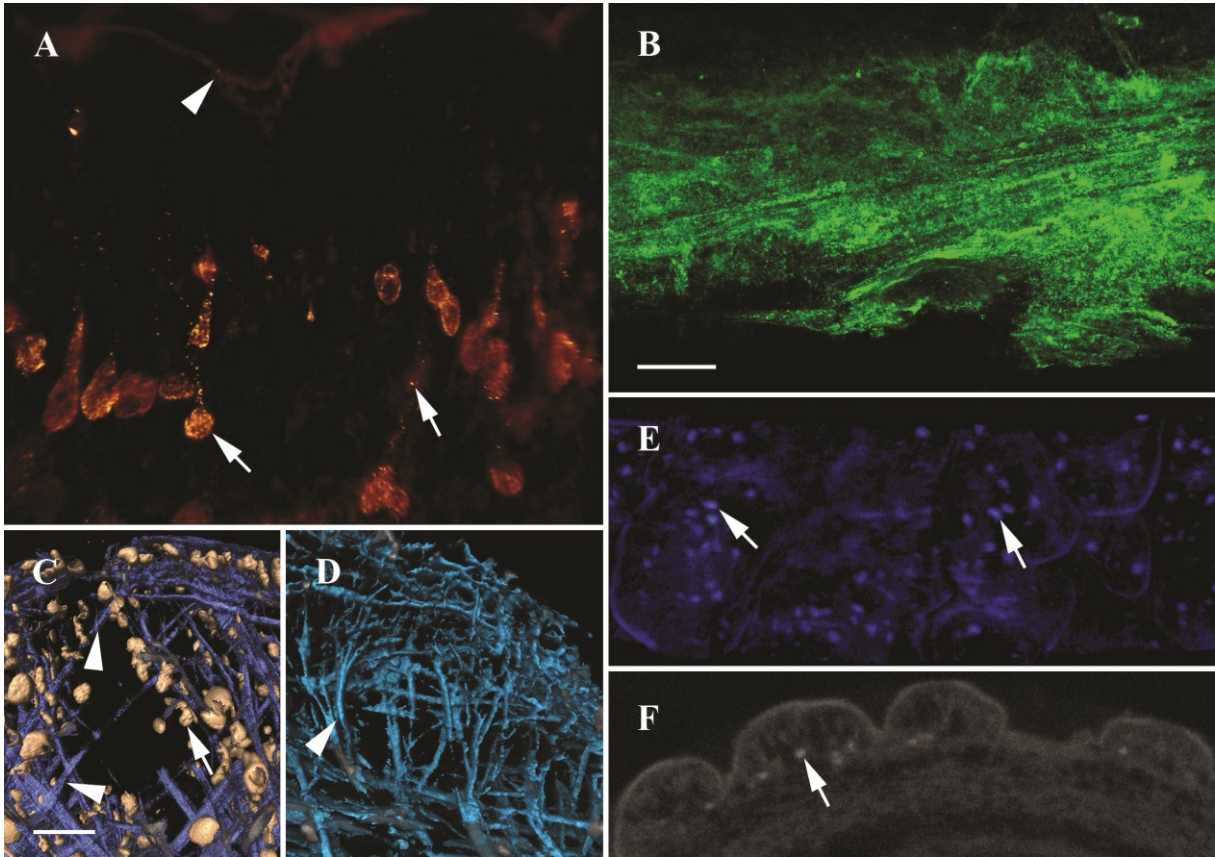


Figure 8

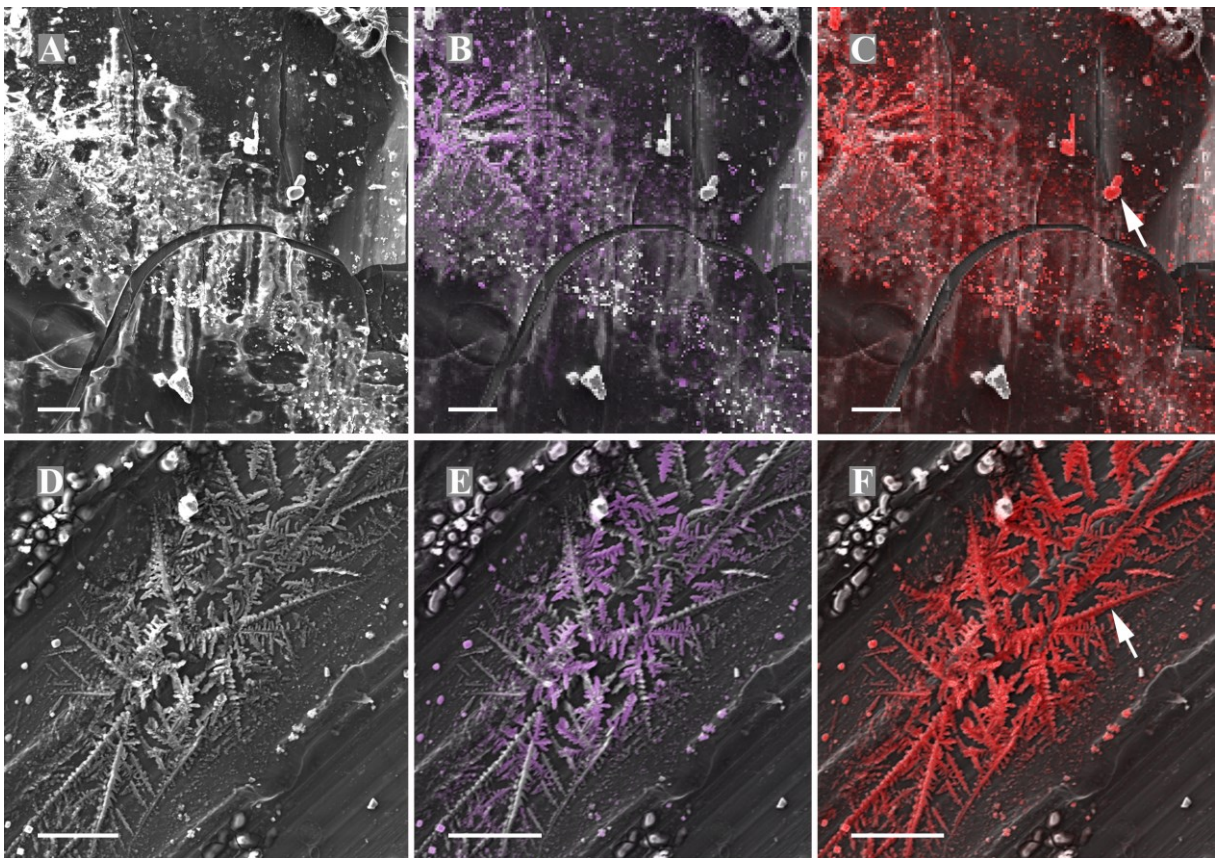


Figure 9

Helix pomatia

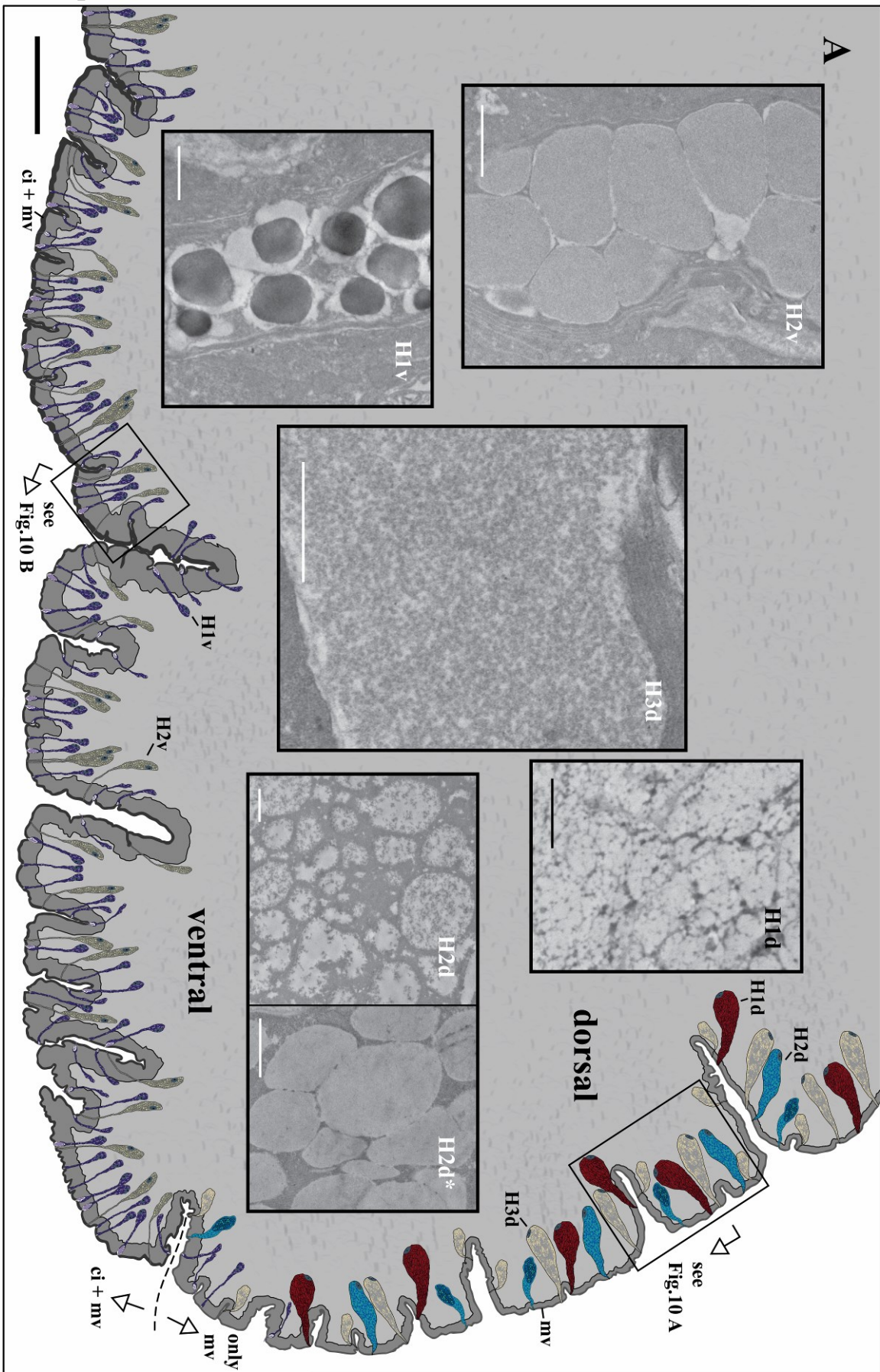


Figure 10

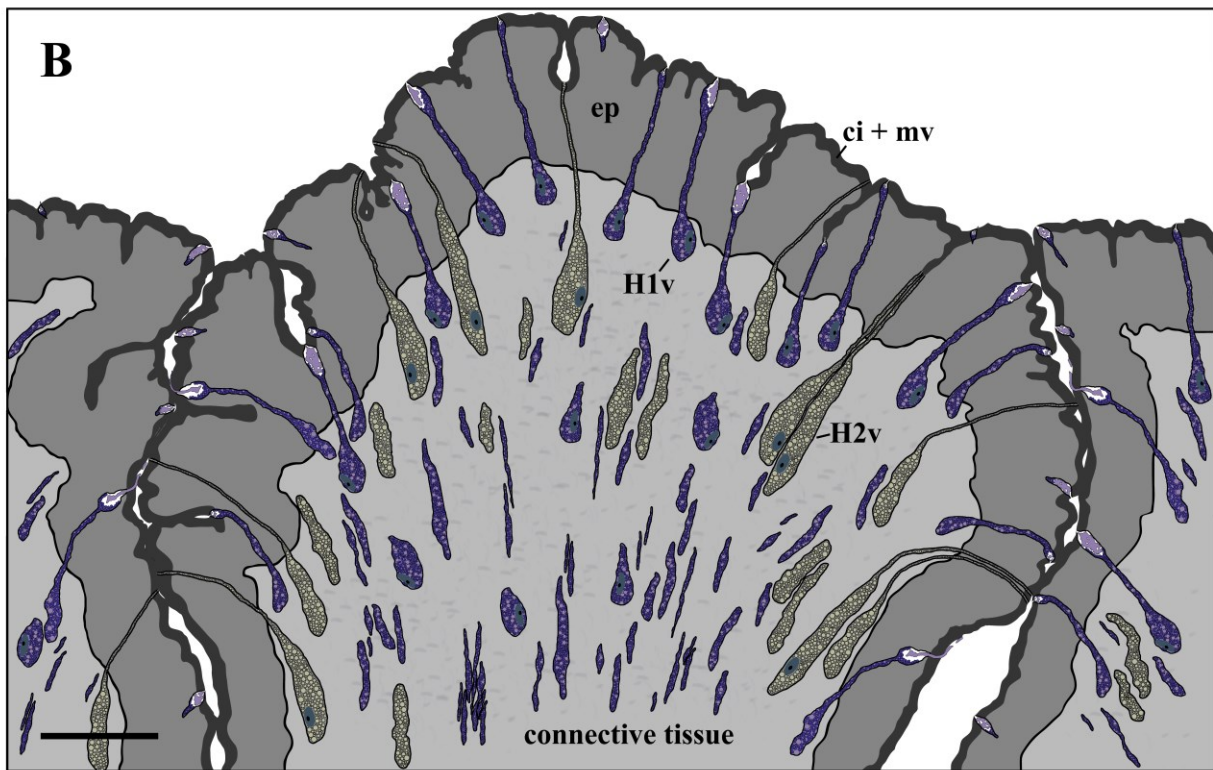
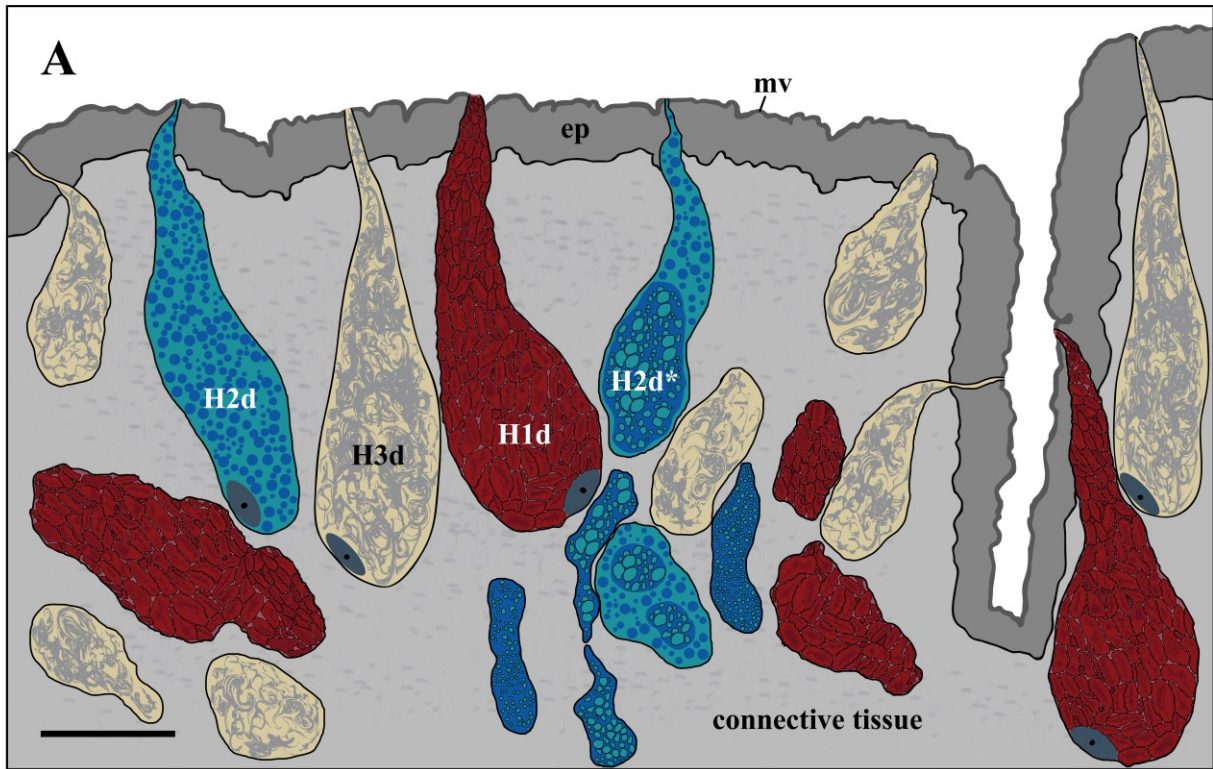


Figure 11

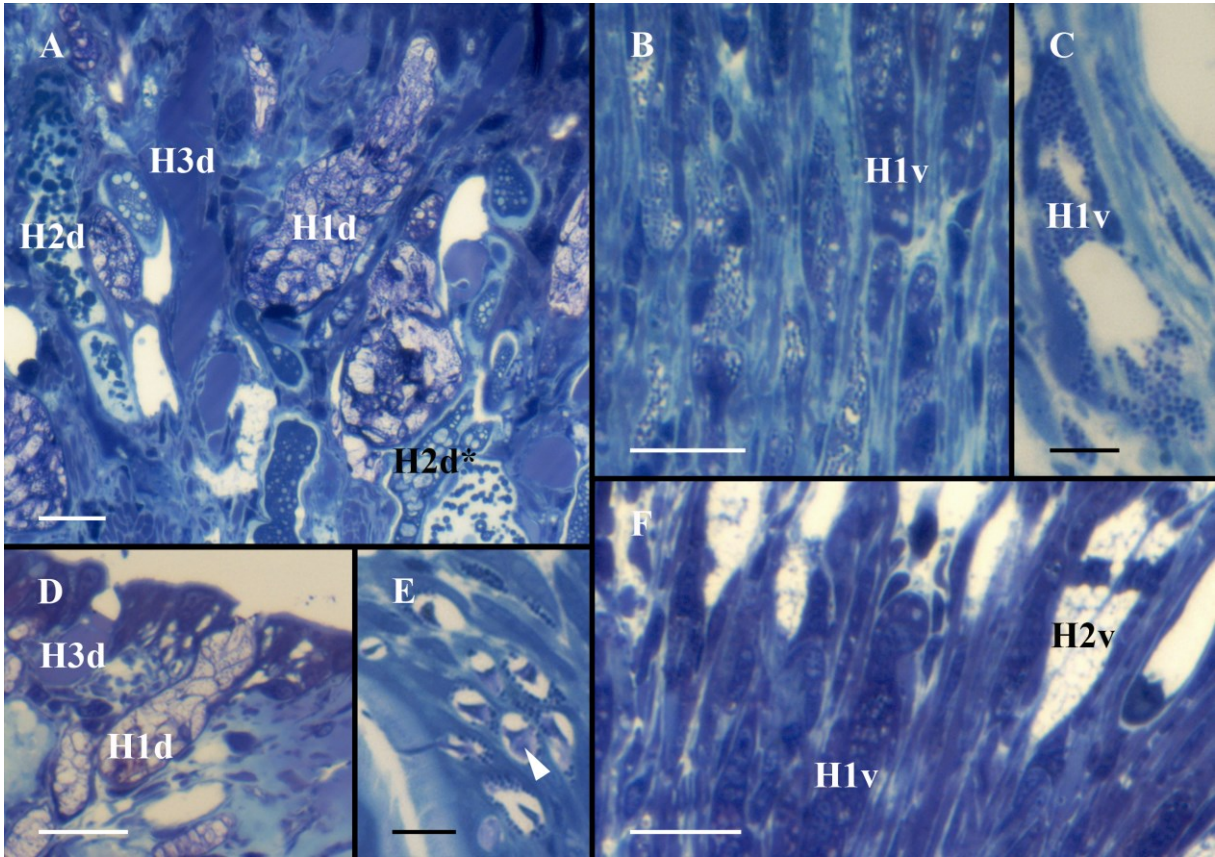


Figure 12

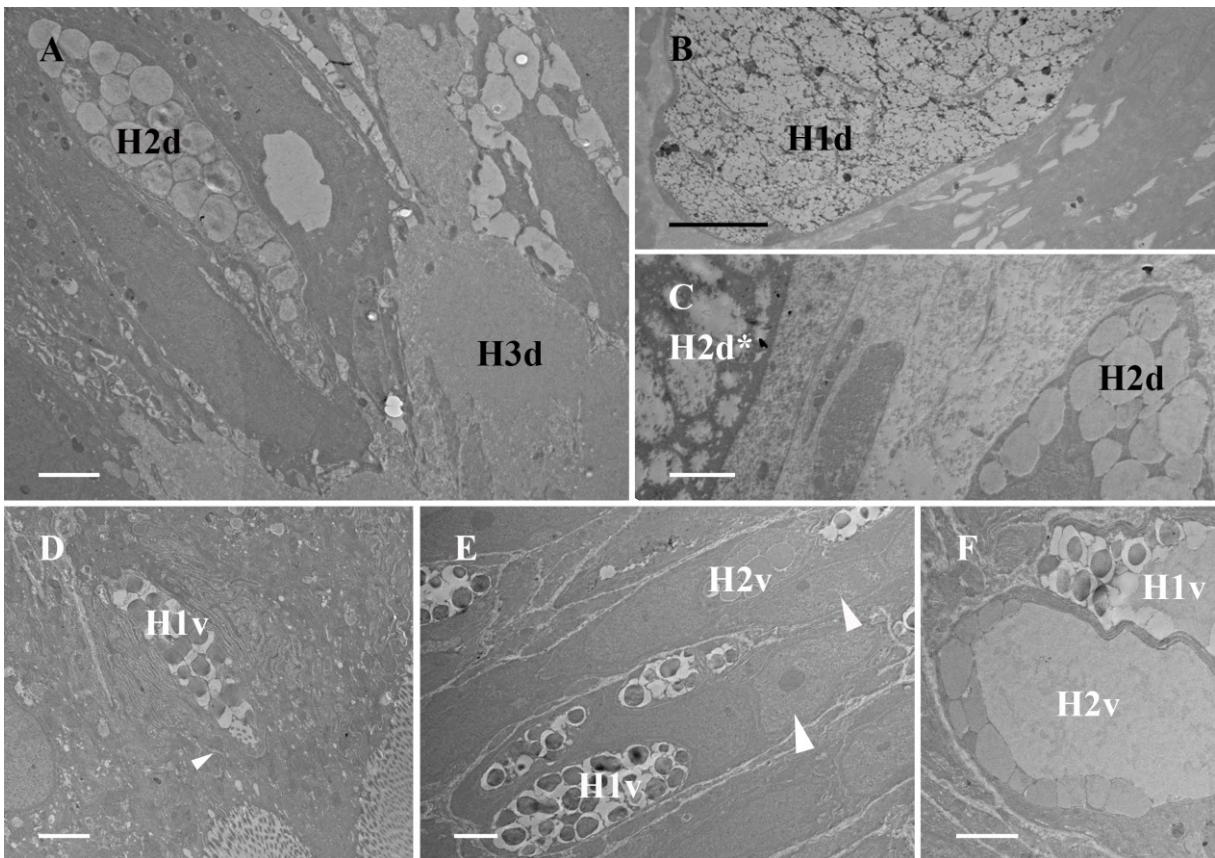


Figure 13

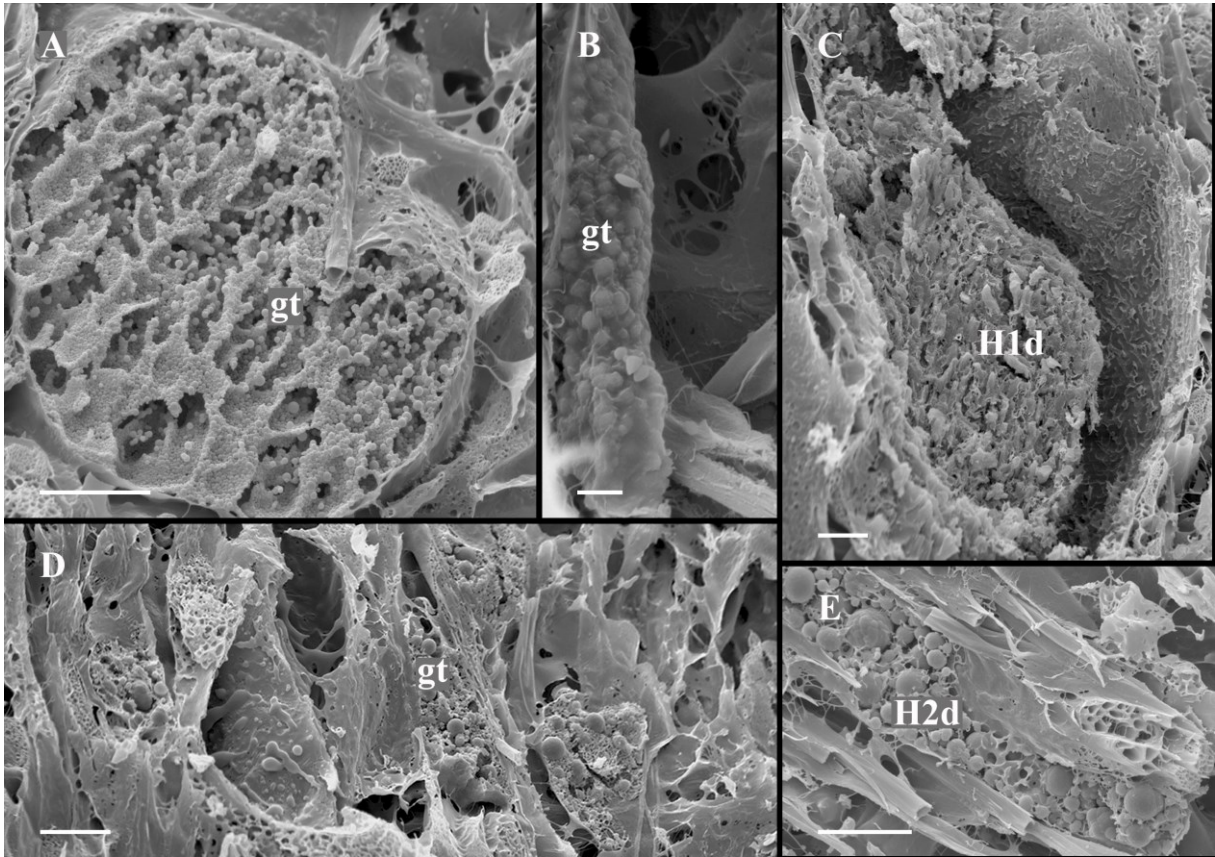


Figure 14

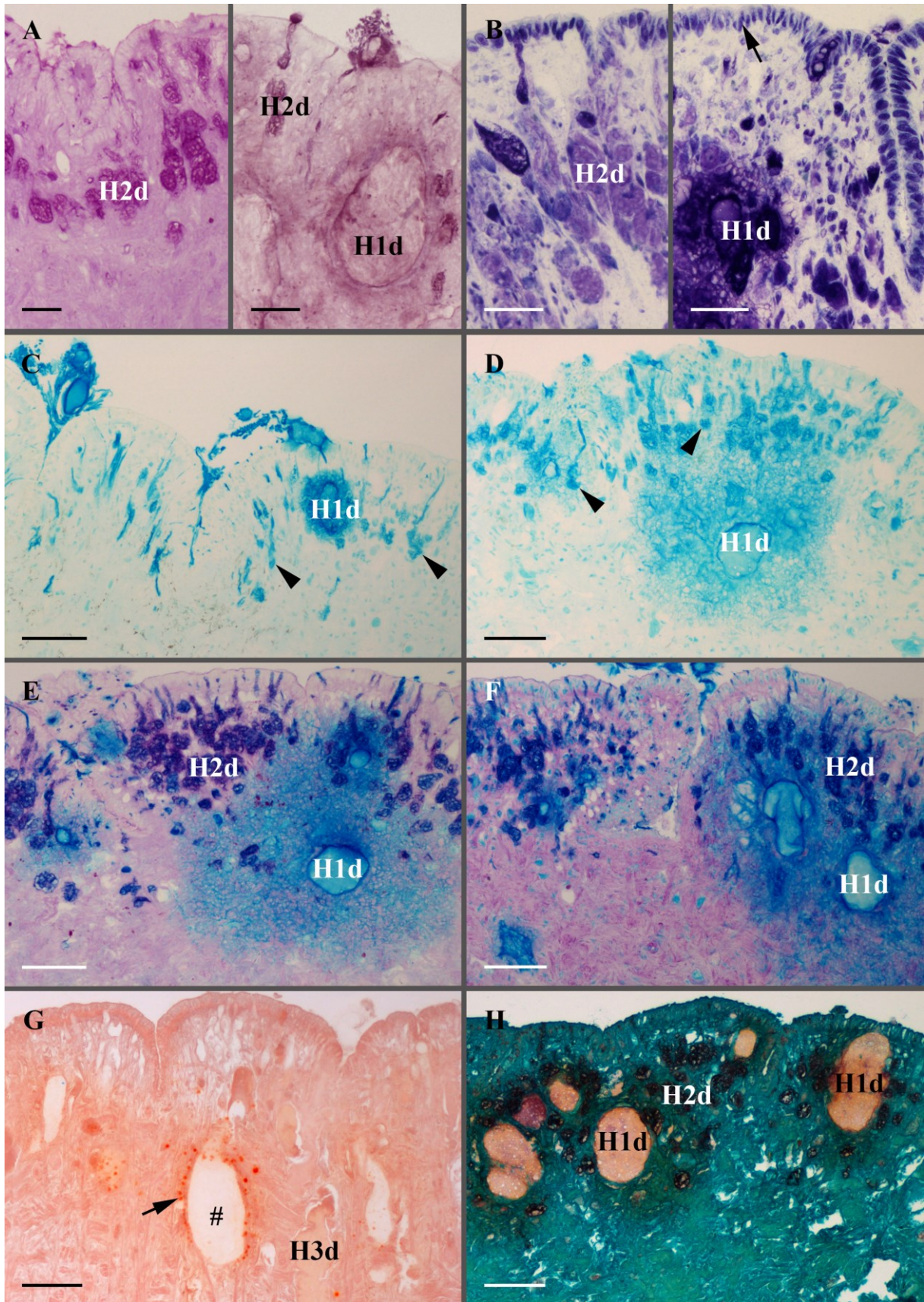


Figure 15

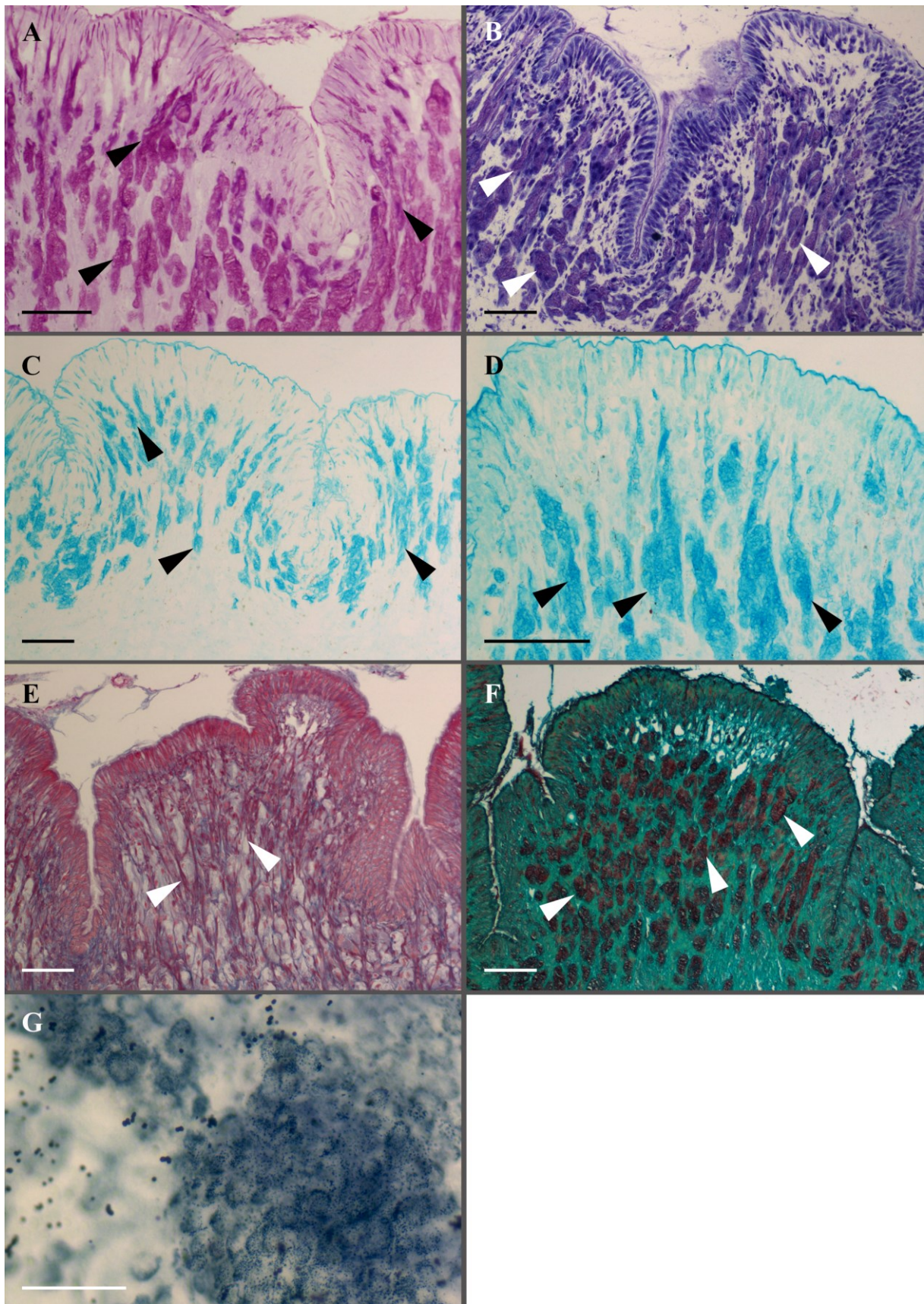


Figure 16

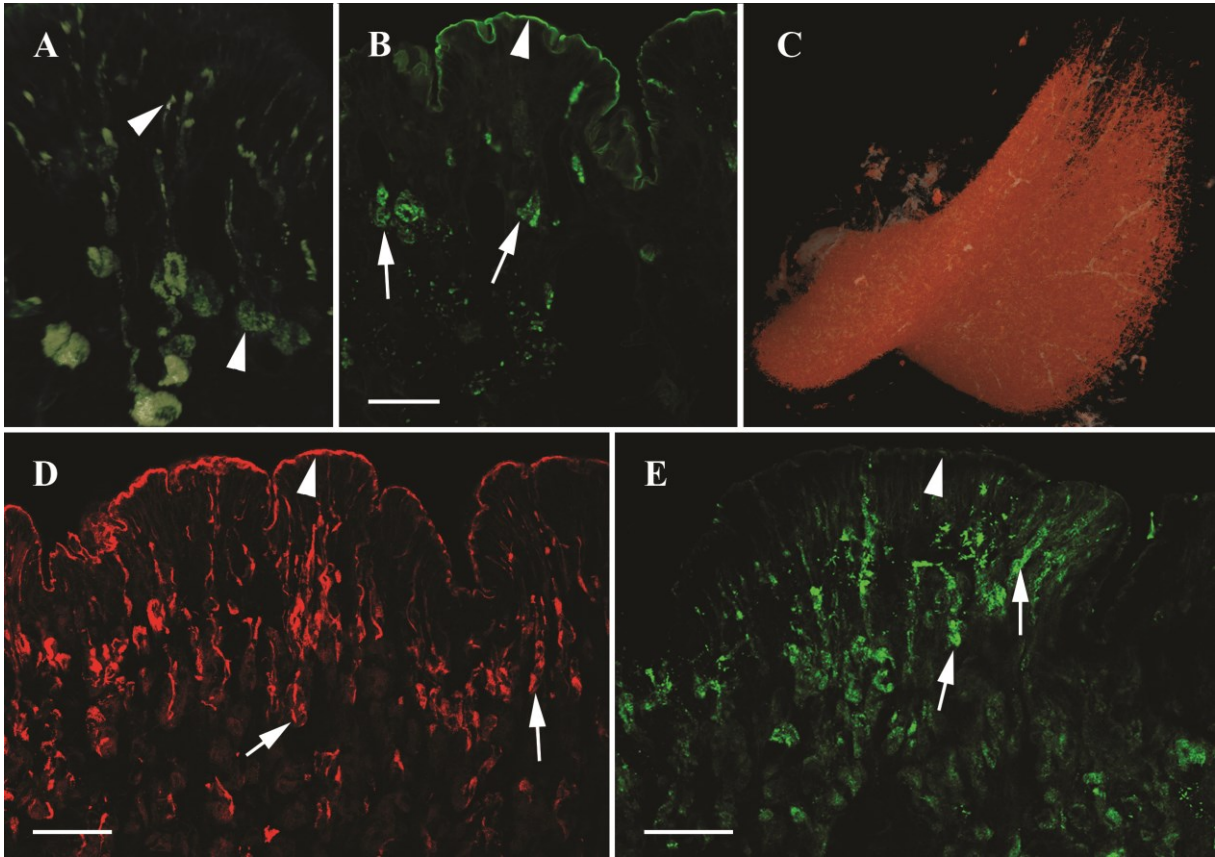


Figure 17

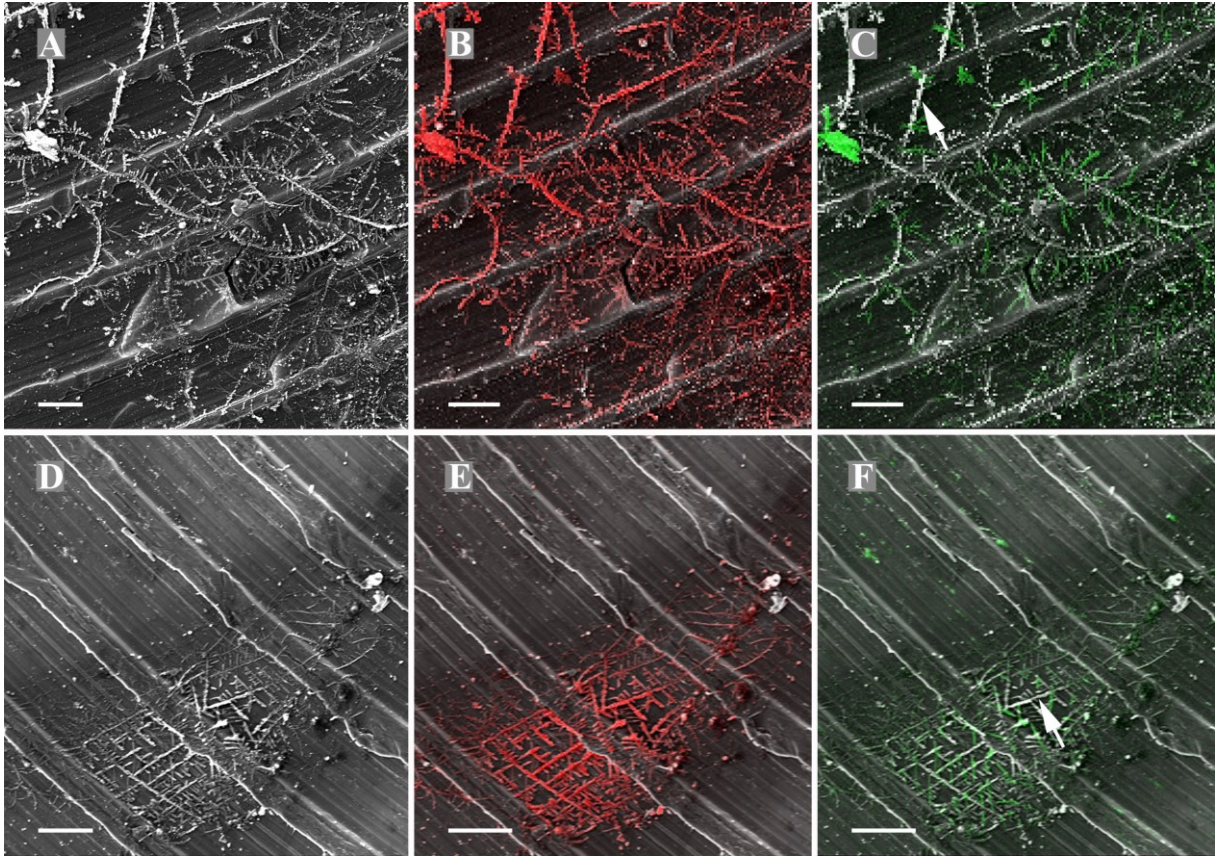


Figure 18

Cepaea hortensis

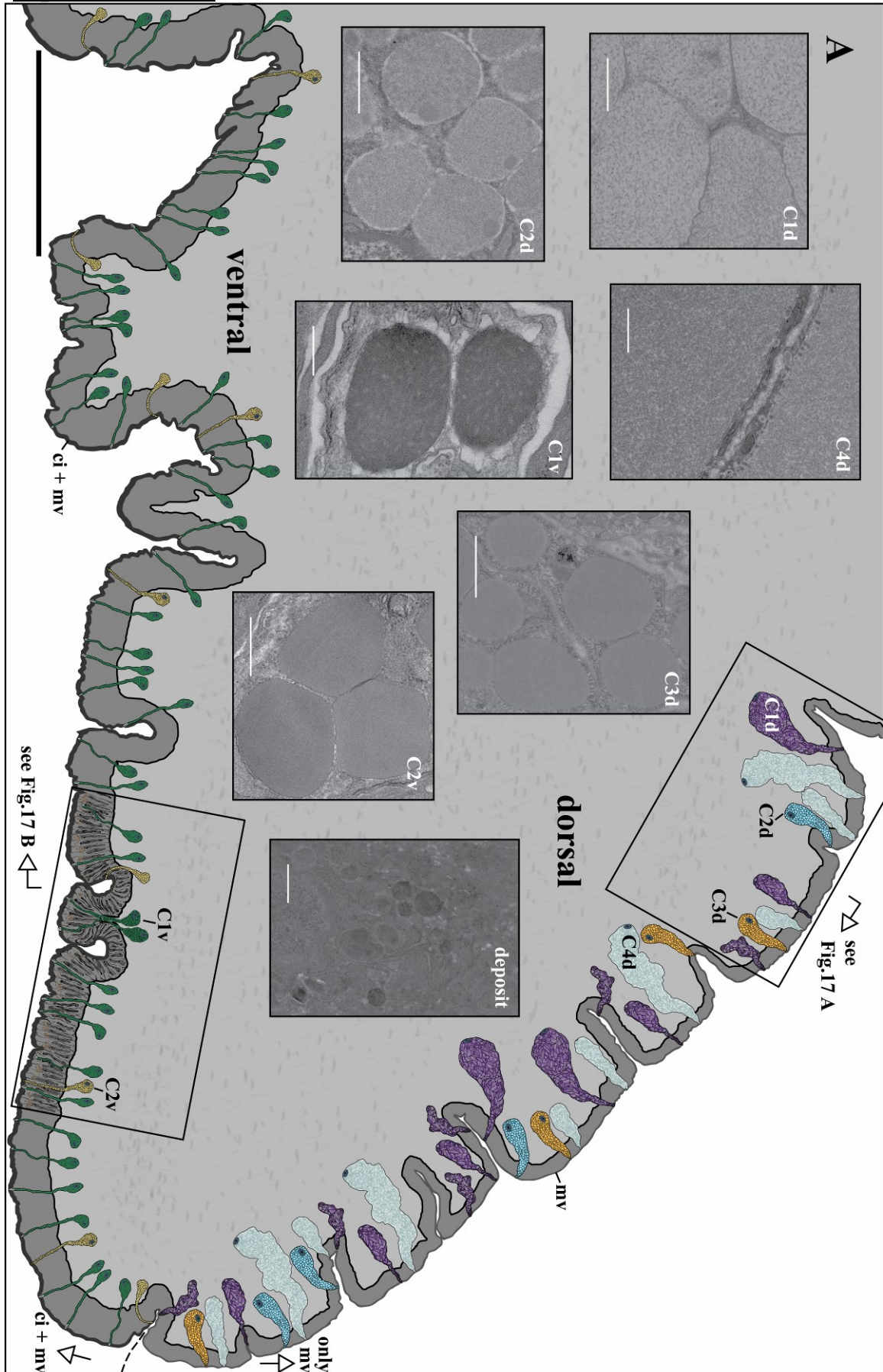


Figure 19

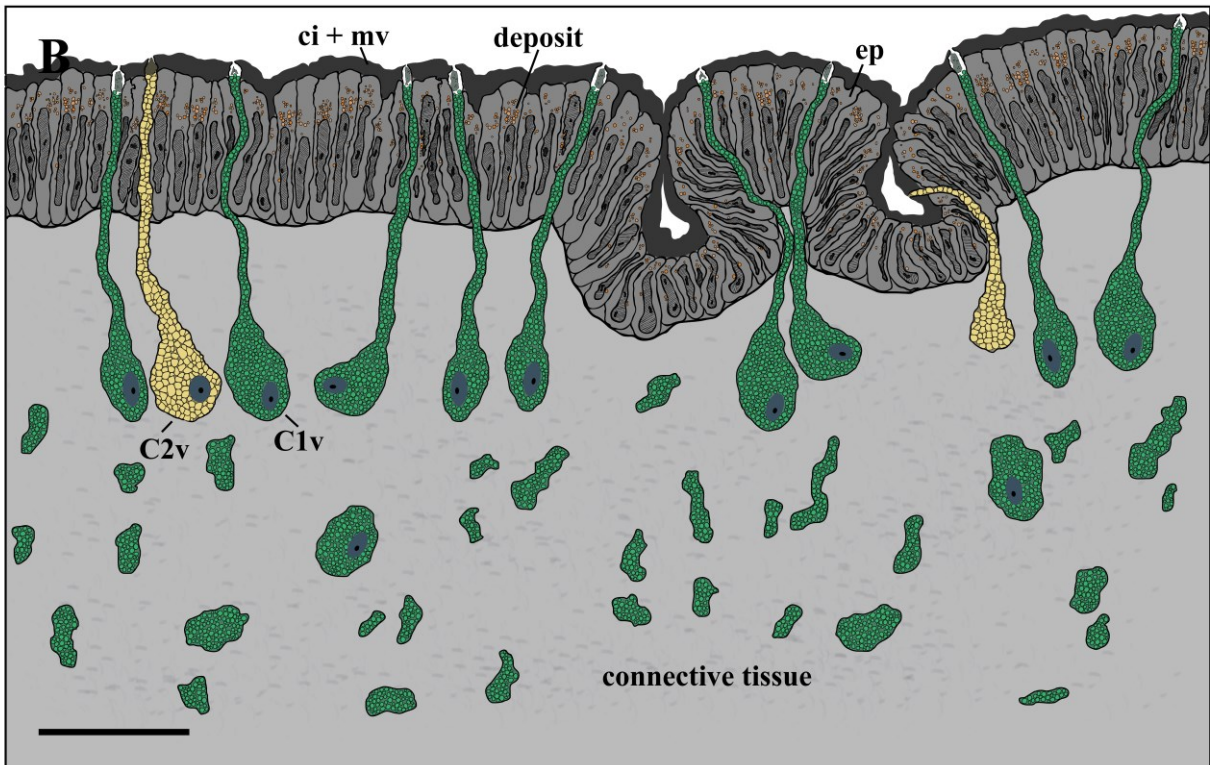
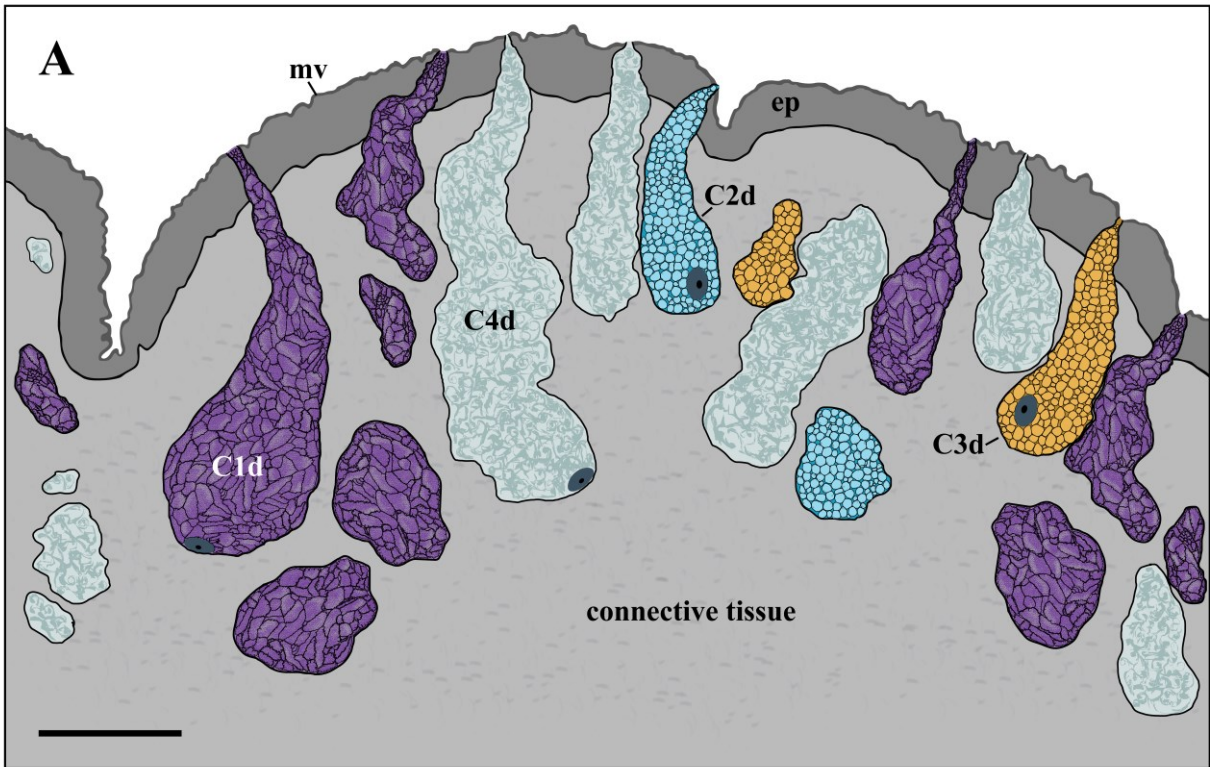


Figure 20

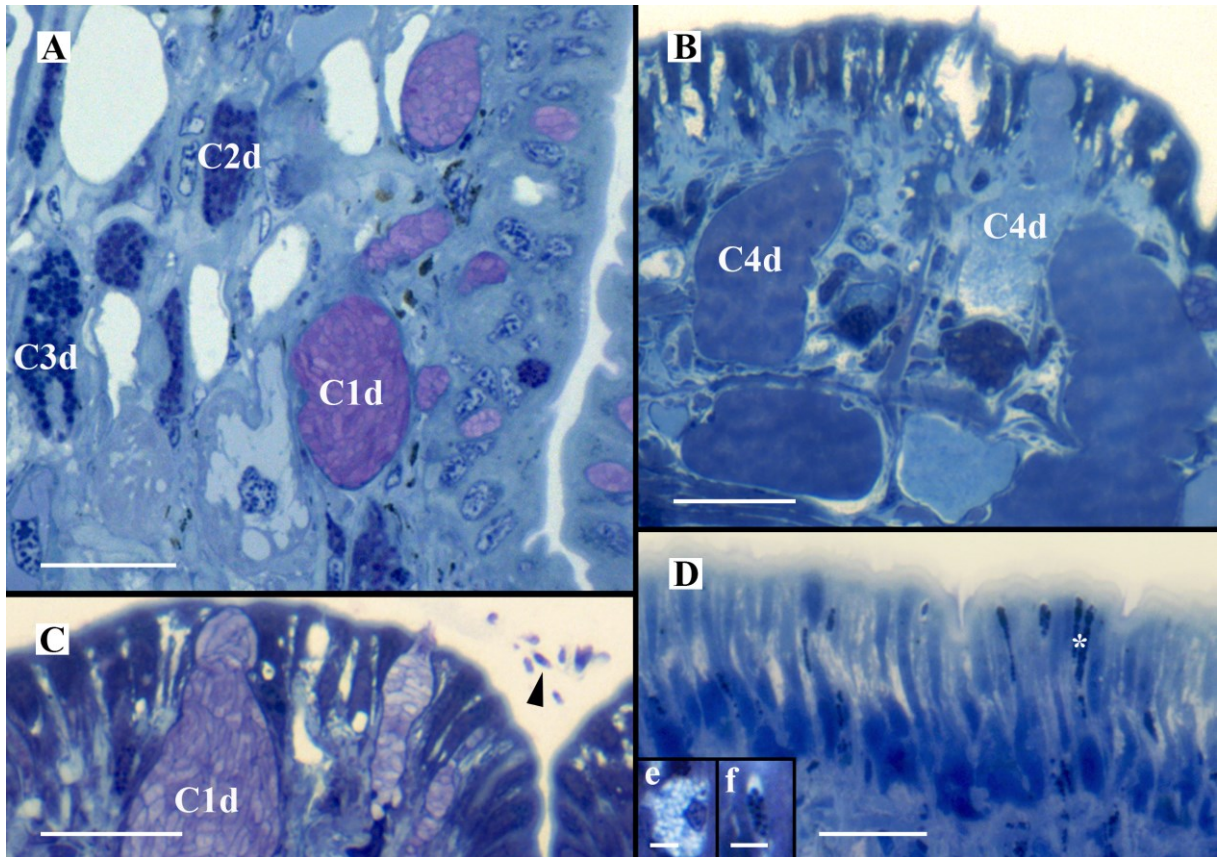


Figure 21

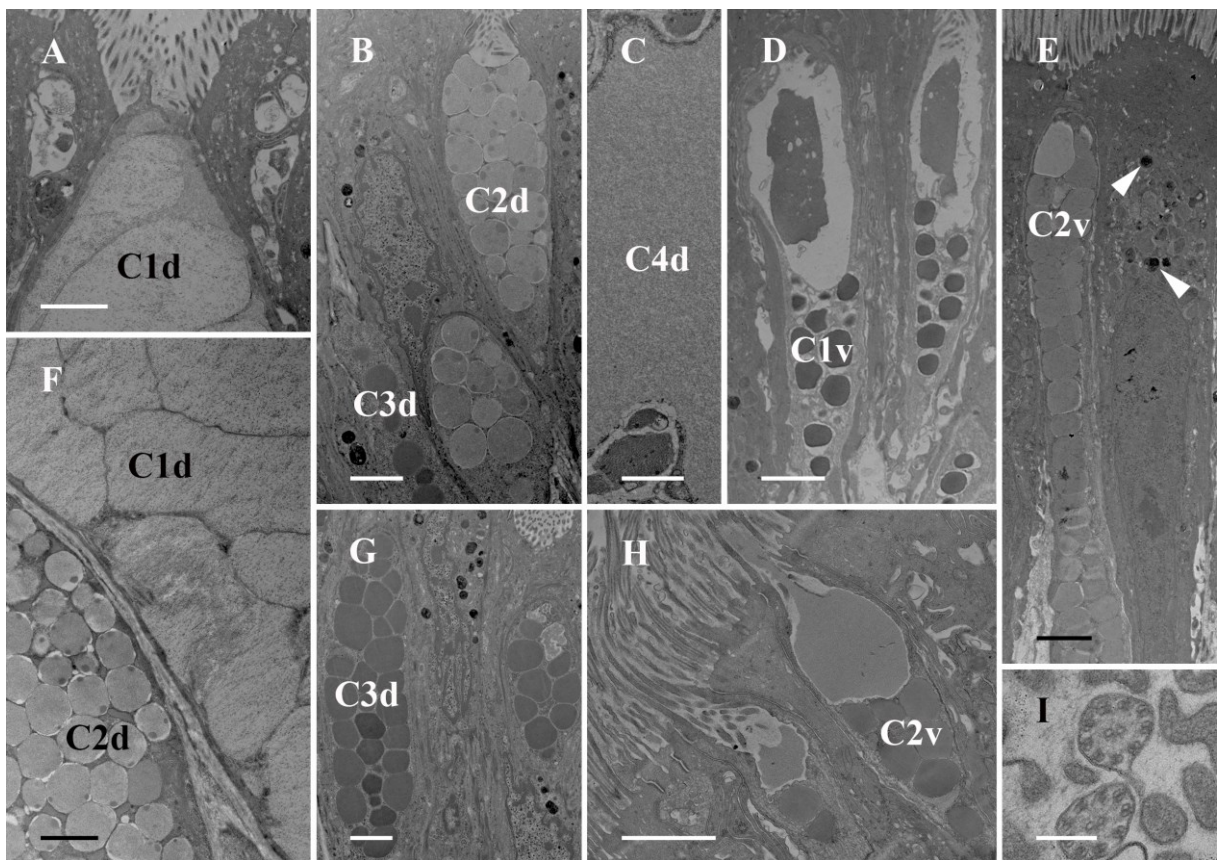


Figure 22

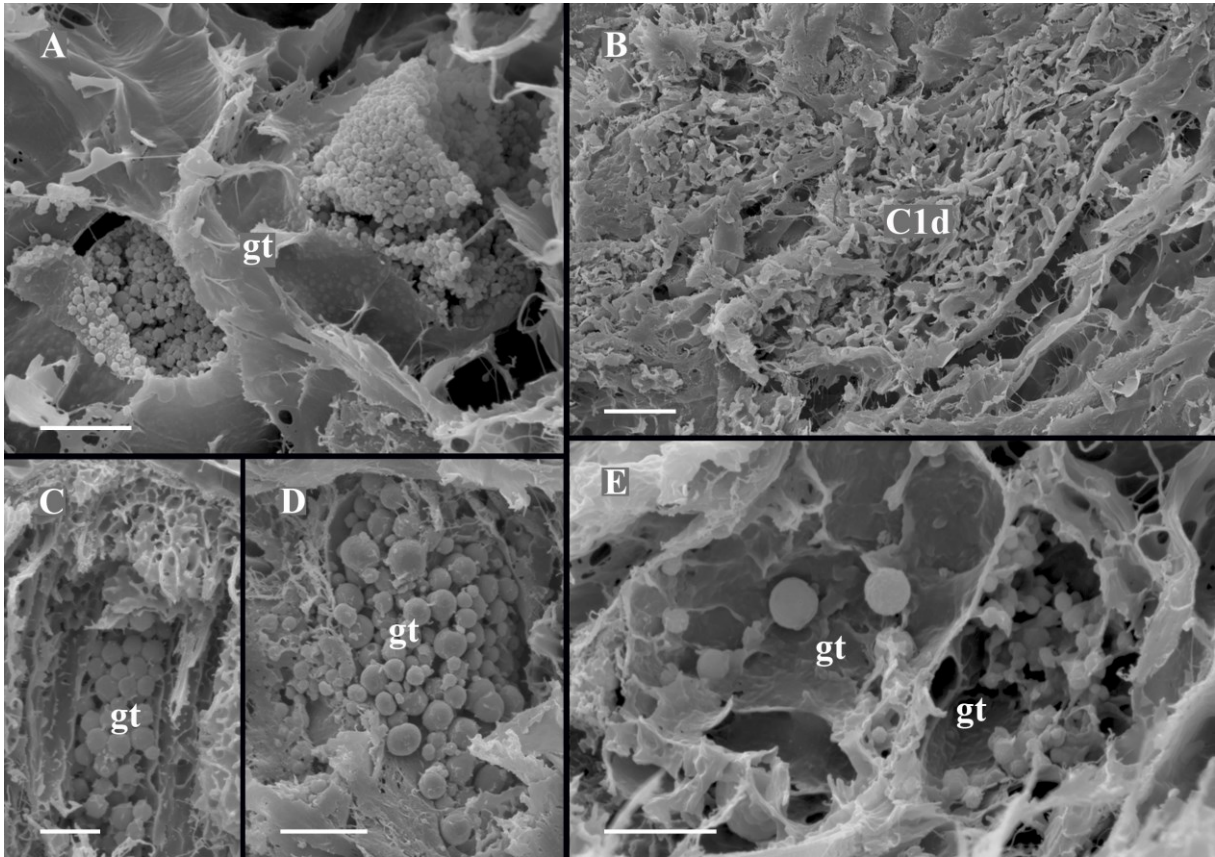


Figure 23

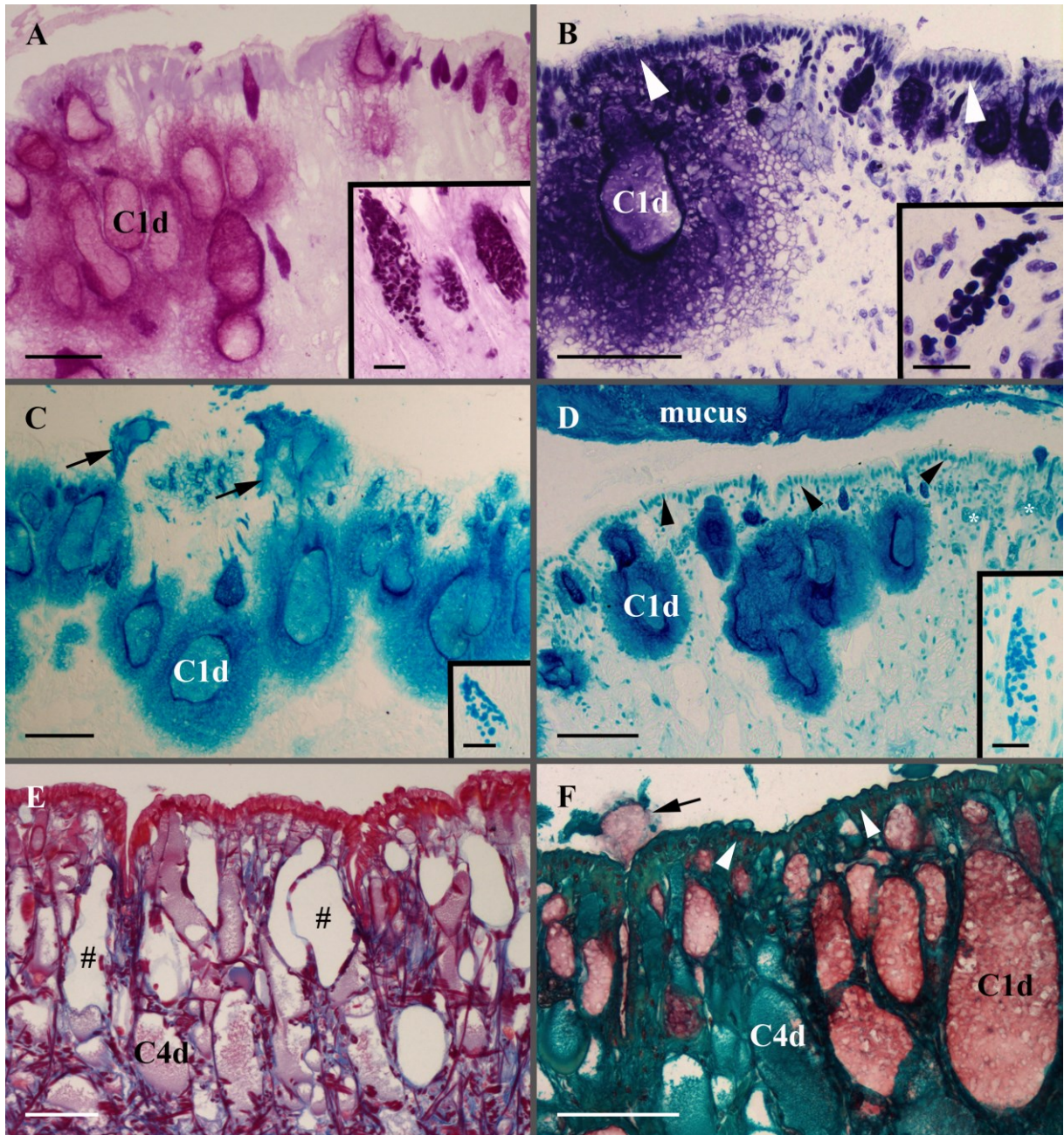


Figure 24

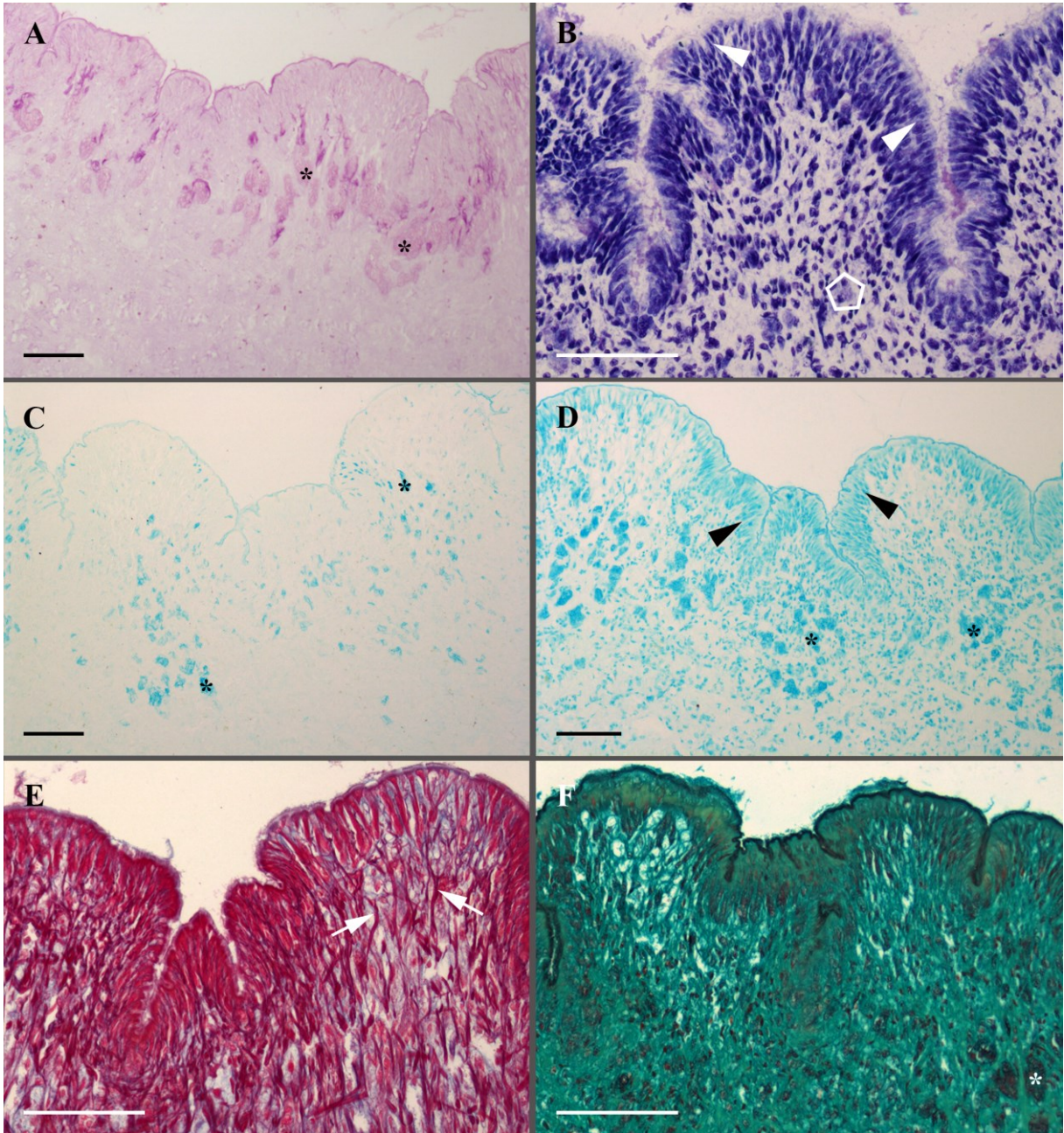


Figure 25

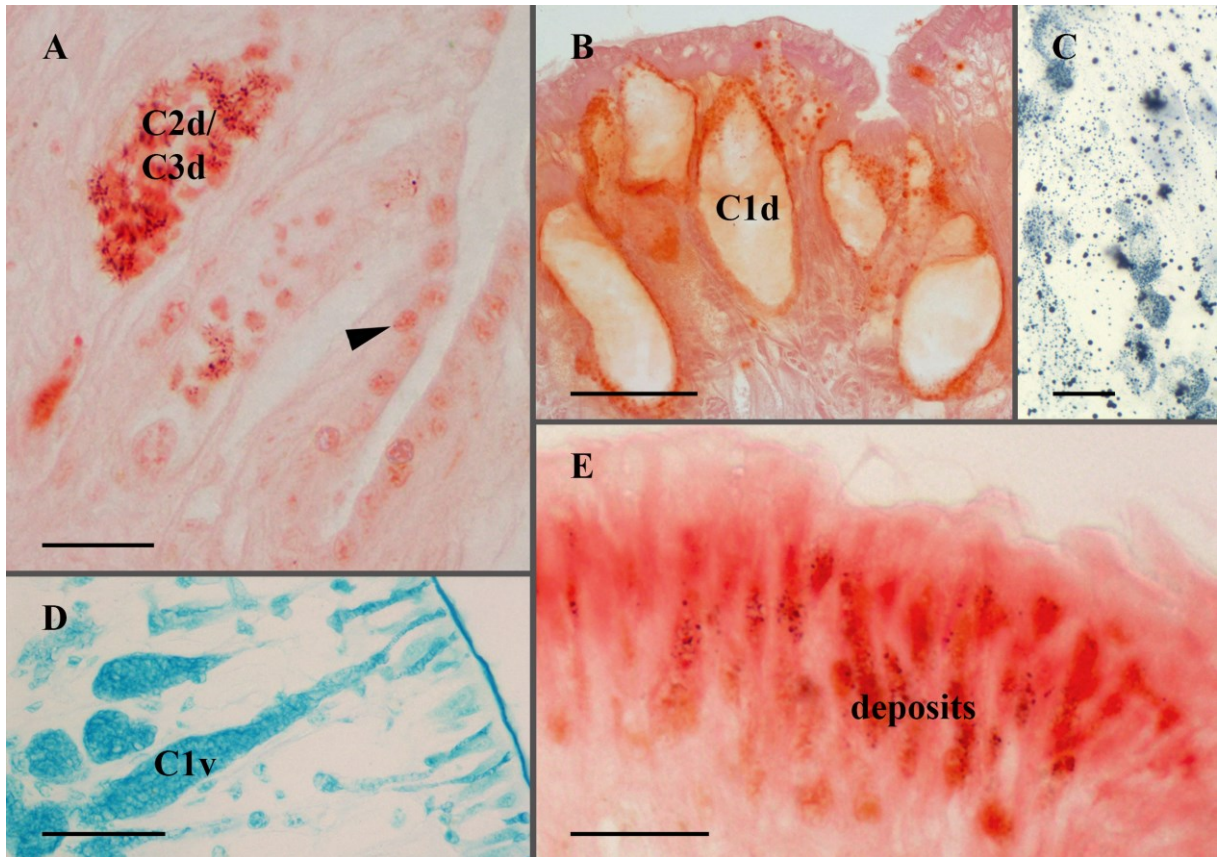


Figure 26

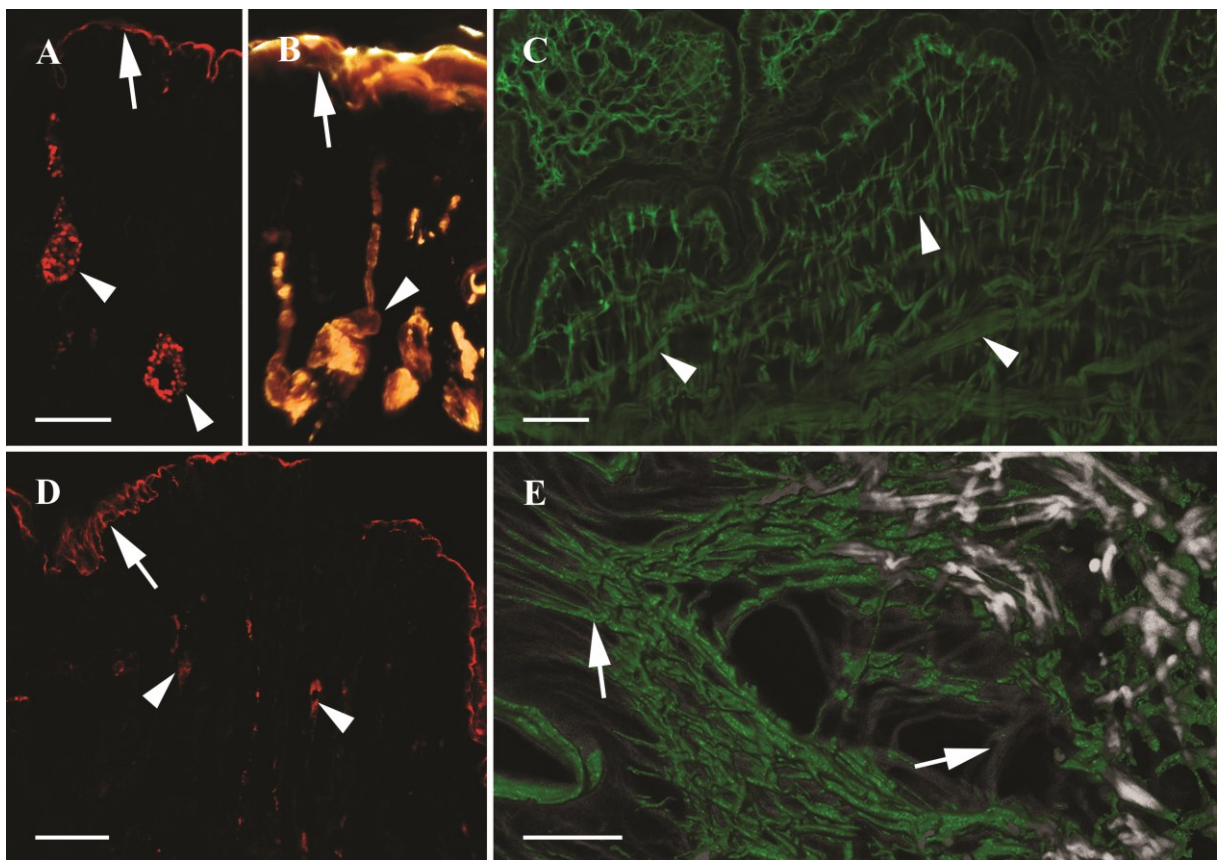


Figure 27

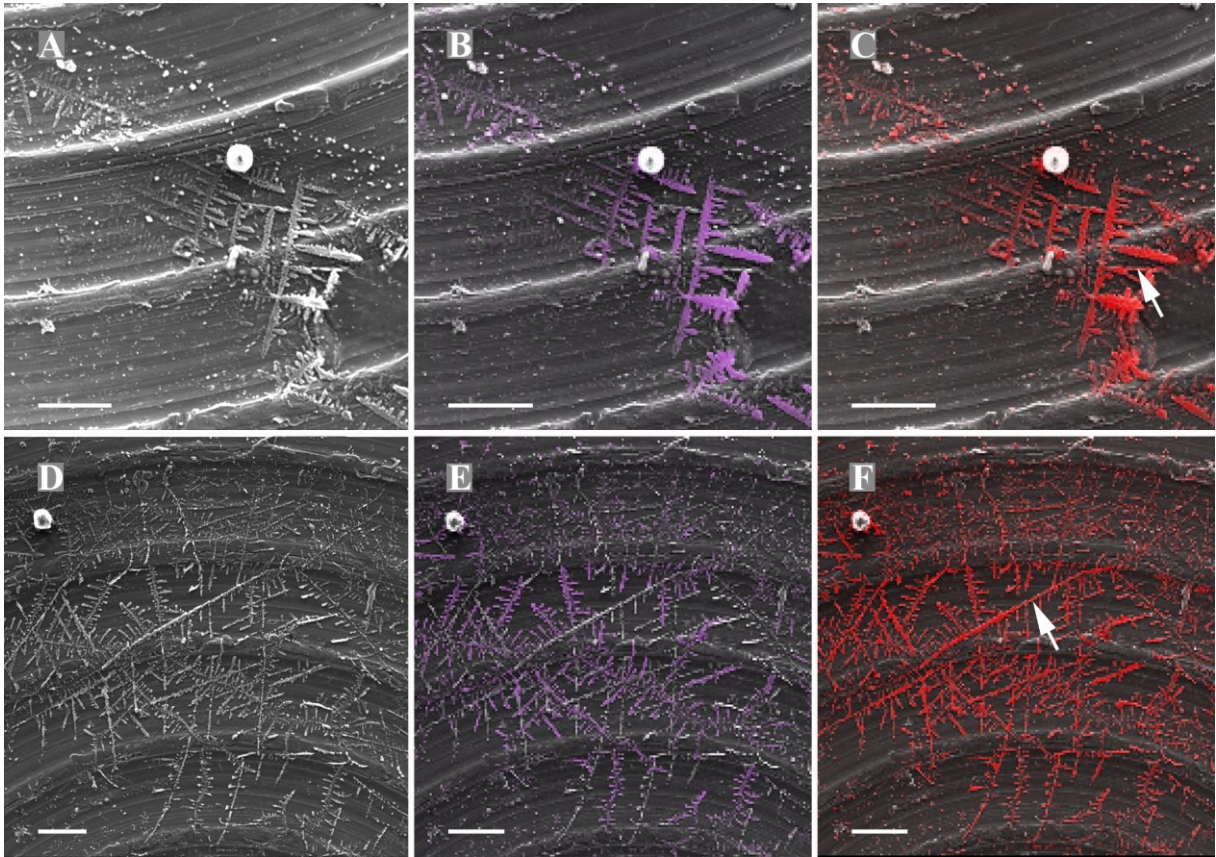


Figure 28

12 APPENDIX

12.1 Zusammenfassung

Gastropoden produzieren eine große Menge Schleim in der Fußregion, der unterschiedlich verwendet wird, sei es zur Verteidigung gegen Räuber, zum Anheften oder zur Fortbewegung. In den verschiedenen Regionen des Fußes sind eine Vielzahl von Drüsenzelltypen vorhanden, die eine unterschiedliche chemische Zusammensetzung ihrer Sekretion aufweisen. Obwohl viel über die Drüsenzellen in den marinen Vertretern dieser Tiergruppe bekannt ist, fehlt ein Vergleich dieser Drüsen bei terrestrischen Gastropoden.

In dieser Studie erfolgte eine vergleichende ultrastrukturelle Studie zur Morphologie der Pedaldrüsen bei *Arion vulgaris*, *Helix pomatia* und *Cepaea hortensis*, darüber hinaus wurden die Sekretinhalte histochemisch und immunocytochemisch analysiert.

Die Daten zeigen eine große Vielfalt hinsichtlich der Anordnung der verschiedenen Zelltypen und der Schleimzusammensetzung innerhalb und zwischen den drei Arten: Im dorsalen Fußbereich von *Arion vulgaris* konnten fünf Drüsentypen unterschieden werden, die alle saure Proteine (positive Alcianblau Färbung) aber keinen Zucker (negative PAS-Färbung) aufweisen. Im ventralen Fußbereich sind nur vier Drüsentypen sichtbar, wobei hier ausschließlich saure Mucopolysaccharide (Protein und Zuckermischung) vorkommen.

Helix pomatia weist drei dorsale Drüsentypen auf, die eine unterschiedliche Zusammensetzungen aufweisen. Im ventralen Bereich wurden hingegen nur zwei Drüsenzelltypen identifiziert, die wie *Arion vulgaris* ebenfalls saure Mucopolysaccharide synthetisieren.

Die Charakterisierung des Fußes von *Cepaea hortensis* zeigt vier dorsale und zwei ventrale Drüsentypen, von denen die meisten positiv für Zucker und saure Proteine sind. Nur ein dorsaler Drüsenzelltyp reagiert auf keinen applizierten histochemischen Test.

Die Untersuchungen zeigen deutliche Unterschiede hinsichtlich der Anzahl und Zusammensetzung der Drüsen innerhalb der Arten und zwischen den Spezies. Es stellt sich die Frage, ob diese morphologischen und chemischen Unterschiede auf unterschiedliche Funktionen und/oder verschiedenen Lebensbedingungen der Tiere zurückzuführen sind.